GÖTEBORGS UNIVERSITET
Institutionen för geovetenskaper
Avdelningen för oceanografi
Geovetarcentrum

TIDAL PROPAGATION AND WATER EXCHANGE IN MTWAPA CREEK, KENYA

Charles Magori

ISSN 1400-3821

B70
Projektarbete
Göteborg 1997

Postadress
Geovetarcentrum
S-413 81 Göteborg

Besöksadress
Geovetarcentrum
Guldhedsgatan 5A

Telefon
031-773 28 00

Telefax
031-773 28 49

Earth Sciences Centre
Göteborg University
S-413-81 Göteborg
SWEDEN

TIDAL PROPAGATION AND WATER EXCHANGE IN MTWAPA CREEK, KENYA

Charles Magori
Kenya Marine and Fisheries
Research Institute
PO Box 81651
Mombasa, Kenya

Earth Science Centre
Department of Oceanography
S-41381 Gothenburg
Sweden

Thesis for Master of Science degree in Physical Oceanography at the
University of Gothenburg
May 1997

CONTENTS

ABSTRACT

Mtwapa creek is a tropical tidal creek, surrounded by mangrove dominated mudflats. The entrance channel is long and deep. Time series of sea levels, current velocities and water temperatures were used to study tidal propagation within the creek and at the entrance. Harmonic and spectral analysis showed that the tide is typically semi-diurnal ($F \approx 0.2$). A 10% decrease in the semi-diurnal tidal range including appearance of shallow water tides towards the inner end of the creek indicate a weak choking caused by channel friction.

Maximum channel currents lag high tide by 3.45 hours and there is a phase lag of 15-20 minutes in maximum sea level between the creek and the entrance. The currents show an assymetry of ebb-dominance, with both higher ebb velocities and shorter ebb periods, which fits with the topography of this creek.

Water exchange was calculated from salinity measurements in the uppermost part of the creek. The residence time for water in that end was estimated to 12 days, compared to 3 days as an average for the whole creek. This latter estimate was derived from heat flux and temperature measurements. The water exchange is totally dominated by the tide. Therefore, regarding an average of 3 days there is a considerable variation between spring and neap.

A simple linear model [Pugh, 1979] was applied to the creek. The model assumes that except near slack water at the mouth where local acceleration is important, the principal force balance within the channel is between the pressure gradient force and bottom friction. Though it has several shortcomings, it describes the inner tide reasonably well. It also estimates the rate of dissipation of tidal energy.

1. INTRODUCTION

1.1 General

Coastal lagoons can be classified as (1) choked, (2) restricted or (3) leaky, based on the degree of water exchange between the lagoon and ocean (Kjerfve and Magill, 1989). In this study, we will focus on a slightly choked coastal lagoon (or tidal creek) which is shallow and features a restricted tidal exchange with the coastal ocean. Choked lagoons are usually connected to the ocean through a single, long and narrow channel and they are sensible to pollution, sediment infilling and eutrophication.

The objective of this paper is to study tides and the mechanism controlling water exchange in Mtwapa creek, a coastal lagoon 20km north of Mombasa on the Kenyan coast. A map of the creek is shown in Fig 1. This lagoon differs from many other coastal lagoons; It is less wide and open and apart from the thick mangrove areas around the creek, it is surrounded by hill landscape. At low tide it takes the form of a creek with tributaries. Still it has much in common with the lagoons. There are several hotels and fishing clubs in the outer part. It faces problems like pollution, habitat destruction and an increasing pressure from growing populations cutting woods and thereby presumably increasing risks for, among others, erosion problems. Effluents from a prison located at the creek is disposed into the creek and this is not only degrading the water quality, but is also endangering the marine life. The importance of these environmental problems has led to this study.

Knowledge of water exchange is essential for environmental studies. An effective exchange of water between a coastal lagoon and the open sea improves the water quality and reduces enviromental risks. We are using measurements of tides, salinities, temperatures and currents including a simple model to predict water movements and exchange between the creek and the ocean. The model can also be used to predict changes

in circulation caused by altering the geometry of the channel by eg. dredging or widening. This is important as such changes may have implications with respect to fisheries, navigation, water quality and other lagoon characteristics (Kjerfve and Knoppers, 1991).

1.2 The Problem

Along most coastlines, the tides are recognized as the main agent responsible for water exchange between coastal lagoons and the continental shelf waters. Other agents responsible for exchange are fresh water input, windstress and air pressure fluctuations. In areas of strong tides however, these are often of less importance.

When a tidal wave enters a lagoon which is connected to the open sea by a narrow channel, the amplitude of the lagoon tide is reduced as friction limits the water velocity in the channel and reduces the volume of water that can be exchanged during the tidal cycle. The reduction in lagoon tide amplitude relative to the ocean is referred to as choking (Stigebrandt, 1980).

Studies on tidal propagation within and into channels and lagoons have received attention from several authors. Pugh (1979) developed a model for the tidal response by assuming linear bottom friction in the connecting channel of an atoll system. Stigebrandt (1980) studied choking due to a narrow channel by assuming a Bernoulli acceleration upstream of the channel and a dynamic balance within the channel between bottom friction and along channel pressure gradient. He further assumed a dissipative jet downstream of the channel. Brown and Trask (1980) concluded, like Stigebrandt, that bottom friction and pressure gradient dominates within the channel, and studied that case. Robinson *et al.* (1983) applied a numerical model based on non-linear long wave propagation theory to demonstrate the tidal behaviour in the Fleet, a long narrow bar-built tidal lagoon. He showed that the different constrictions in the fleet act as low-pass filters

allowing longer period tides and surges to penetrate but damping out higher frequencies like the semi-diurnal tide. If the channels are very shallow, fortnightly tides may appear because of the variation of friction in the spring neap cycle (Robinson *et. al.* 1983; Hill, 1994).

Dronkers, 1964, Parker, 1984 and Godin, 1988 derived analytical solutions for channel flows with friction. These authors studied tidal propagation as qualitatively similar to that of a damped second order wave equation. Several investigators have estimated friction coefficients using current measurements and sea level data from shallow tidal inlets (e.g. Heath, 1981; Swift *et al.* 1983; Smith, 1985; Odido, 1994; Rydberg and Wickbom, 1996).

This paper focuses on channel flow with special emphasis on the tidal propagation in Mtwapa creek which is connected to the ocean through a long and narrow but relatively deep channel. Mtwapa creek is likely to be choked according to the definition of Kjerfve and Magill (1989). There is no earlier information on the physical oceanography of this lagoon.

Sea-level, current, temperature and salinity measurements have been used to

i). study water exchange by determining volume fluxes, residence times and channel friction coefficient, and

ii). apply a one dimensional analytical model developed by Pugh (1979) to predict water elevation in the creek.

1.3 The Study Area

Mtwapa creek ($3^0$55'S, $39^0$45'E) is a shallow tidal, mangrove fringed lagoon system located on the Kenyan coast in the Western Indian Ocean (Fig 1). The creek is connected to the ocean through a long narrow channel. There are reef linings on the entrance.

Inwards from the channel is a shallow, lagoon type bay. The channel itself is approximately 6km long and 300m wide. It has a mean depth of 10m. The maximum depths are about 20m near the entrance but decrease to approximately 3m upstream of the bridge as shown in Fig 2.

The tide in this area is semi-diurnal, with a spring tidal range of 3.2m and a neap tidal range of 0.8m as observed in Mombasa (Pugh, 1979). This means that the surface area of the channel varies from 1.43 x $10^6 m^2$ to 1.82 x $10^6 m^2$ during low water spring (LWS) and high water spring (HWS) respectively while the surface area of the bay varies from 2.15x$10^6 m^2$ to 11.8x$10^6 m^2$ during low water spring (LWS) and high water spring (HWS) respectively. The total volume of water in the creek including the channel ranges from 1.24x$10^7 m^3$ at LWS to 3.80x$10^7 m^3$ at HWS.

Large areas of the bay are exposed during low water spring (LWS). Further upstream are mangrove swamps along the wide intertidal flats and they are an important forestry resource. Most of the mangroves are partially flooded at each high tide. A seasonal river Mto Mkuu enters into the system. The annual mean monthly discharge of Mto Mkuu river is 0.3$m^3 s^{-1}$ (Fig4; Norconsult, 1975).

Geology

The geology of the study area is characterised by a raised reef towards the Indian Ocean, behind which are various sedimentary formations, generally running parallel to the coast. The estuary of the Mtwapa creek cuts through the reef complex into sandy and shelly beds of sedimentary formations. Below the sea-bed are partly coral rocks and partly deposits of sand, silt, clay and mud, as seen from Fig 3 (Norconsult, 1975).

Meteorological conditions

The area experiences a tropical climate characterized by the monsoon seasons. In general, the climate is hot and humid throughout the year. The shifting monsoons result in two distinct dry seasons and two rainy seasons. The South-East Monsoon (SEM), related to the long rains, occurs from April to October and the North-East Monsoon (NEM), which causes the short rains, occurs from November to March. The monsoon transitional stages occur in late October and mid April respectively. The annual rainfall in Mtwapa region averages 1000mm, with maximum precipitation occurring during the long rains (Meteorological Dept., 1995). The annual average air temperature is 27^0C. The relative humidity averages 80%. The rates of evaporation are 6mm per day during the dry season and drops to less than 2mm per day during the wet season. Precipitation and river discharge are shown in Fig 4.

The surface winds in the coastal region of Kenya are dominated by the two distinct monsoons. The winds of the NEM are markedly influenced by a land-sea breeze. They blow at an average wind velocity of about 6m/s. The winds of the SEM are stronger and to a lesser degree influenced by the land-sea breeze. They blow mostly to the North with an average velocity of 7.5m/s (Norconsult, 1975).

The East African Coastal Current (EACC) flows northwards throughout the year but differs markedly in its characteristics between the two monsoons. During the NEM, along Kenya, the EACC converges with a weaker southward flowing Somali Current. The convergence zone of these currents constitutes the root of the Equatorial Counter Current. During the SEM, a large portion of the Equatorial Current is moved northward via the powerful Somali Current along Kenya and Somalia and is absorbed eastward by the southwest monsoon current (Duing and Schott, 1977).

2. MATERIAL AND METHODS

2.1 Field Measurements

Sea level measurements were made by means of two MicroTide pressure gauges. One was deployed at Claudio, near the entrance of the channel, from 9 January to 14 February 1997 and the other within the creek, halfway upstream (Creek station) from 9 to 24 January 1997 (see Fig 1). The pressure gauge at the Creek station was moved to the Oceanic station and deployed there for two days from 27 to 29 January 1997. The instruments which have a precision of ± 1.5cm were set to measure and record water level and temperatures at 5 minutes interval.

Within the same period, a Sensordata SD 6000 recording current meter was moored near the entrance at the Claudio station at a depth of 10m. This instrument measured current velocities and water temperature at 5 minutes interval. The current meter has an accuracy of ±2cm/s and $\pm 5^0$ respectively. However, due to the risk of loosing instruments, the current measurements were carried out during short periods only; two days during neap tide, from 18 to 20 January 1997 and three days during spring tide, from 7 to 10 February 1997.

Salinity data was collected twice a month from June to September 1996 at the Claudio station, at the Bridge and within the Creek, far upstream. Hourly salinity measurements were conducted at Claudio on 29th September 1996 for 24 hours. These measurements were carried with an Aanderaa in situ Salinity-Temperature sond. The sond measures salinity with an accuracy of ± 0.1 PSU. Results are shown in Table 5.

Detailed echo soundings were made along the channel in order to determine its geometrical characteristics. The results are shown in Fig 2. The depths are referred to the

lowest astronomical tide at Mombasa for 1996, which was 0.1 m above the Admirality Chart Datum.

2.2 Raw data treatment

To make it possible to compare data from the two tide gauges, a calibration was carried out immediately after data collection by putting the instruments into a water tank at the same level and then varying the water level in the tank. A calibration coefficient of 0.98 was determined. The pressure data from the Claudio tide gauge was adjusted for the difference. Further, the observations from the tide gauge at Claudio was compared to the simultaneous observations from the Oceanic tide gauge. The purpose of doing this was to find out whether the water levels observed at Claudio reflected the Oceanic water levels. The difference was small ($\leq$ 2% difference). We decided that there was no need to make any adjustments, and that the data from the Claudio station could be regarded as representative for the oceanic sea level.

The pressure recorded by the tide gauges, P, is the sum of the atmospheric pressure, p_a, and the pressure of the overlying water column, as given by the hydrostatic equation $P = p_a + \rho gh$, where ρ is the density of sea water; g is acceleration due to gravity and h is the height of the water column. The pressure P, is in [PSI] units and was converted to [m] by multiplying by 0.69. The air pressure was assumed to be constant during the observations and was reduced from the raw data in order to obtain the relative sea level heights. Time series of sea levels at the Claudio and Creek stations are shown in Fig 5.

In order to level the tide gauge at Claudio and the one at the Creek station, the times for slack water was determined from the current meter data. We assumed that at slack water in the channel, the sea levels at the Claudio and Creek sites were equal. Having done this levelling, the sea level figures from the two stations were put together in two plots,

Fig 6 a,b, comparing spring and neap elevations. We also carried out float drouge measurements at three sites on the bridge for the same purpose. It then turned out that there was a considerable variation across the channel in time for slack water, up to one hour between the north and the south side. However, we were not able to handle the results at this stage.

The tide gauge data from Claudio and Creek stations was subjected to spectral and least square harmonic analysis (chapter 2.3) using a Matlab programme written by Cederlöf (1995). The programme was run using fourteen harmonic constituents. It includes eight principal harmonic constituents and six so called shallow water tides (See Table 1). The results are shown in Table 3. Fig 7 a-c and Fig 8 a-c show computed and residual tides for Claudio and Creek station respectively, according to the harmonic analysis program. Classification of tides was made according to the form number, F, as shown in Table 2. Tidal statistics based on results from the harmonic analysis were computed for both stations and the results are presented in Table 4.

The main directions of the currents in the channel were determined by plotting directions versus current velocities. The plot is shown in Fig 11. The velocities were then resolved into along channel and cross channel components. We also resolved the current velocities into east-west and north-south components. Longitudinal and lateral variations of currents in the channel are compared in a scatter plot shown in Fig 12.

The bathymetry of the inlet channel was mapped with an echosounder during the surveys in 1996. The results of bathymetry measurements are shown in Fig 2. The bathymetry of the creek itself, however was never carried out in detail. Thus we used a seachart indicating tidal channels, minimum and maximum sea levels and mangrove areas, to sketch on a hypsographic curve for the creek. The result is shown in Fig 14 a,b also showing volume versus depth. Although the mean volumes and areas might be reasonably

well estimated by this crude method, the details are far from good and to obtain improvements on modelling and in relating channel velocities to tidal heights for the future, it is necessary to make a better bathymetry.

2.3 Theory on Harmonic analysis

Harmonic analysis is a mathematical method for extracting sinusoidal components of specific frequencies from e.g. a sea level record. In this case, it is based on the ''method of least squares''. Instead of fitting a straight line to the data by varying its slope and intercept, a set of cosine (or sine) curves with given frequencies ω are fitted by varying *amplitudes* and *phases,* minimising the sum of deviations from the original curve.

Given a time series Z(t) of data points, its tidal part can be expressed as a combination of sine and cosine functions (cf. Cederlöf, 1995).

$$Z(t) = \sum_k a_k \sin(\omega_k t) + \sum_k b_k \cos(\omega_k t)$$

The values of a_k and b_k can be calculated for given frequencies, ω_k by minimising the sum of squares of the differences between the assumed function and the given time series Zn.

Least square fit requires that

$$f(a_k, b_k) = \sum_{n=1}^{N} \left(z_n - \sum_k a_k \sin(\omega_k t_n) + \sum_k b_k \cos(\omega_k t_n) \right)^2 = \text{minimum}$$

This requirement is satisfied by

$$\frac{\partial f}{\partial a_i} = 0 \quad \text{and} \quad \frac{\partial f}{\partial b_i} = 0 \; ; \quad i = 1,2,\ldots\ldots\ldots,k$$

where

$$\frac{\partial f}{\partial a_i} = -2 \sum_{n=1}^{N} \cos(\omega_i t_n) \left(z_n - \sum_k a_k \sin(\omega_k t_n) - \sum_k b_k \cos(\omega_k t_n) \right) = 0$$

$$\frac{\partial f}{\partial b_i} = -2 \sum_{n=1}^{N} \sin(\omega_i t_n) \left(z_n - \sum_k a_k \sin(\omega_k t_n) - \sum_k b_k \cos(\omega_k t_n) \right) = 0$$

The above equations can be rewritten as

$$\sum_k a_k \sum_{n=1}^{N} \sin(\omega_k t_n)\cos(\omega_k t_n) + \sum_k b_k \sum_{n=1}^{N} \sin(\omega_i t_n)\sin(\omega_k t_n) = \sum_{n=1}^{N} Z_n \sin(\omega_i t_n)$$

$$\sum_k a_k \sum_{n=1}^{N} \cos(\omega_i t_n)\cos(\omega_k t_n) + \sum_k b_k \sum_{n=1}^{N} \cos(\omega_k t_n)\sin(\omega_k t_n) = \sum_{n=1}^{N} Z_n \cos(\omega_i t_n)$$

This can be simplified by introducing the notation

$C_{in} = \cos(\omega_i t_n)$, $S_{kn} = \sin(\omega_k t_n)$

$$\sum_k a_k S_{kn} C_{kn} + \sum_k b_k S_{in} S_{kn} = \sum_n Z_n S_{in}$$

$$\sum_k a_k C_{in} C_{kn} + \sum_k b_k C_{in} S_{kn} = \sum_n Z_n C_{in}$$

which gives a system of 2k equations with 2k unknowns; a_1 through a_k and b_1 through b_k.

2.4 A one-dimensional frictional model

Consider a lagoon with a surface area A_L connected to the ocean by a narrow channel of length l, depth h, and width w. n_o and n_L are the water level in the ocean and lagoon respectively (See Fig 18). Following Pugh (1979), we assume a dynamic balance in the channel between local acceleration, pressure gradient and bottom friction.

$$\frac{\partial \eta}{\partial x} = -\frac{1}{g}\frac{\partial u}{\partial t} + \frac{G}{g\rho h} \qquad (1)$$

where positive flow is along the x axis into the lagoon and where tidal level changes $\partial\eta$ are ignored compared with the mean depth, h of water in the channel. ρ is the density of sea water ; A_L , l , and w are assumed independent of the tidal level, requirements which are not strictly fulfilled for Mtwapa creek.

Suppose that a linear law of friction applies,

$$G = -K\rho u , \qquad (2)$$

where K is a dimensional friction coefficient. From continuity we have

$$A_L \frac{\partial \eta_L}{\partial t} = whu \,, \qquad (3)$$

Substituting into (2) for u and into (1) for G we have

$$\frac{\partial \eta}{\partial x} = -\frac{1}{g}\frac{A_L}{wh}\frac{\partial^2 \eta_L}{\partial t^2} - \frac{KA_L}{gwh^2}\frac{\partial \eta_L}{\partial t} \qquad (4)$$

If K, w, and h are assumed independent of y, then by integrating along the channel

$$g\eta_o = g\eta_L + \frac{KA_L l}{wh^2}\frac{\partial \eta_L}{\partial t} + \frac{A_L l}{wh}\frac{\partial^2 \eta_L}{\partial t^2} \qquad (5)$$

Suppose that the lagoon sea level is driven by a harmonic variation of ocean level, for example M_2,

$\eta_o = H\cos(\sigma t)$,

then the solution of eq. (4) is :

$\eta_L = \alpha H \cos(\sigma t - \theta)$

where

$$\alpha = (\phi 2 + \mu 2)^{-\frac{1}{2}} \quad ; \qquad \theta = \arctan(\mu/\phi)$$

and

$$\phi = \left(1 - \frac{A_L l \sigma^2}{whg}\right) \qquad \text{and} \qquad \mu = \left(\frac{KA_L l \sigma}{wh^2 g}\right)$$

The above solution represents a damped oscillation with a phase lag.

The average rate of energy dissipation due to the work done against channel friction over a tidal cycle of M_2 is computed using the expression

$$E_{loss} = \frac{\sigma}{2\pi}\int_0^{2\pi/\sigma} Guwl\partial t$$

Substituting for G from (2) and u from (3), the rate of energy loss is

$$E_{loss} = \frac{lA_L^2 \sigma^2 K \rho H_L^2}{2h^2 w} \qquad (6)$$

Pugh (1979) used eq. (6) to calculate the rate of energy loss in an atoll system.

2.5 Water exchange and residence time

The continuity equation for salt within the creek can be written as,

$$\frac{d}{dt}(VS_i) = Q_oS_o - Q_iS_i \qquad (7)$$

Where Q_o - Inflow of oceanic water with salinity S_o

Q_i - Outflow of lagoon water with salinity S_i

V - volume of water with salinity S_i

Assuming that the volume, V is constant, which holds if we average over long periods, Eq. (7) can be written as,

$$V\frac{dS_i}{dt} = Q_oS_o - Q_iS_i \qquad (8)$$

Conservation of volume gives,

$$Q_i = Q_o+Q_f \qquad (9)$$

Where, $Q_f = Q_r+Q_p-Q_e$ is the net fresh water supply to the creek, and

Q_r - river supply of freshwater

Q_p- precipitation over lagoon

Q_e- evaporation over lagoon

Thus,

$$V\frac{dS_i}{dt} = Q_oS_o - (Q_o + Q_f)S_i \qquad (10)$$

Equation (10) can be rewritten as

$$Q_o = \frac{V\frac{dS_i}{dt} + Q_fS_i}{(S_o - S_i)} \qquad (11)$$

From Eq. (11), we can compute Q_o and Q_i which gives the water exchange. The residence time T_{res} can be obtained from the expression;

$$T_{res} = \frac{V}{Q_{max}} \qquad (12)$$

Where Q_{max} = max (Q_o,Q_i)

The residence time was computed on the basis of observed salinities and net fresh-water supply and is discussed below.

3. RESULTS

3.1 Tides

The results from the harmonic analysis are shown in Table 3. They are compared to those obtained by Pugh (1979) which were based on analysis of tides in Kilindini harbour, Mombasa using data from Admiralty tide gauge. The semi-diurnal constituents account for 80% of the water level variations of which M_2 alone accounts for 47%. Comparing the results from Claudio with those from the Creek, it indicates that the amplitudes are reduced by approximately 10% within the creek compared to the Claudio site. There is also a phase lag, which is small however. By comparing the time for high and low water at the two stations, the average phase lag at high water between Claudio and Creek station is 15-20 minutes (Fig 6), while the corresponding difference at low water is 7 minutes, only. In the harmonic analysis results, this is not as evident as in the raw data, probably because the time series for the creek station is too short to give correct results.

A notable feature is the presence of shallow water constituents at the Creek station (Table3). For example, M_4 (3cm), MS_4 (2.5cm), and $2MS_6$ (2cm). No shallow water constituents were seen at the Claudio site. The presence of these constituents at the Creek site indicate slight non-linear interactions between the tide as it propagates through the creek and the bottom bathymetry. However, the non-linear response to tidal forcing is very weak as reflected in the magnitudes of these shallow water tides. In combination they account for 3% of the water level variations inside. The M_4/M_2 ratio is a measure of

the degree on non-linear response to tidal forcing (Aubrey and Speer, 1985). This ratio is 0.034 only.

The form numbers obtained using the formula shown in Table 4 are 0.22 and 0.21 at Claudio and Creek sites respectively, indicating that the tides are typically semi-diurnal. The spring tidal range for Claudio and Creek sites are 3.10 m and 2.81 m respectively while the corresponding neap range is 0.93 m and 0.80 m. The average tidal range is 2.0m and 1.8m at Claudio and Creek stations respectively (Table 4). The observed mean flood and ebb duration at Claudio station is 6.35 hours and 6.17 hours respectively while the corresponding values for the Creek station are 6.58 hours and 6.04 hours, indicating a weak ebb-dominance. These values were obtained from the observed sea levels for both stations averaged over ten tidal cycles during both spring and neap tides.

The computed phase age indicates that spring tides lag local passage of full or new moon by 41 hours, whereas the inequality phase relationships, 31° indicates that the water level inequalities occur in both high and low water (see Table 4). Looking at Fig 5, showing observed sea levels at Claudio and Creek stations, we see that there is a semi-diurnal inequality with successive high waters and successive low waters having different heights. Figs 7c and 8c shows the residual records for the Claudio and Creek stations respectively. For both stations, the residuals are small (~ 20 cm). The residuals could be due to local forcing by windstress and air pressure and at the creek station, where the residuals are occasionally larger, because of a very short sampling period, 17 days, only.

The sea levels at the creek station show a surprising feature during ebb. 2.5 hours before low water, the ebbing (dh/dt) is reduced. There is also a rapid decrease in velocities (Fig 13) associated with this change. This effect is not likely to be caused by the geometry of the channel. In that case we would have expected a continuous decrease of dh/dt as it happens e.g. in Bamburi lagoon (Kirugara, 1997).

Fig 9 a,b show an energy density spectrum computed from sea level measurements. At both stations, the semi-diurnal and diurnal energy peaks are dominating the spectrum. However, at the Creek station, three minor peaks are apparent at the half semi-diurnal periods and other compound tides periods, thus indicating that the shallow water tides contribute some little energy. For both stations, at periods below approximately 10 hours, the spectrum becomes somewhat ragged, and the computed energy density peaks are probably not statistically significant.

3.2 Currents

The current measurements from Claudio near the oceanic side in the outer part of the channel are shown in Figs 10 a,b. Maximum spring velocities were approximately 0.80 ms^{-1} towards 110° during ebb and 0.50 ms^{-1} towards 280° during flood. Average flood and ebb flow directions are seperated by 170° (Fig 11). Due to a malfunctioning compass on the current meter, we were not able to obtain correct directions during neap. However, it was yet possible to determine the periods of in and outflow, from which we estimated maximum velocities of approximately 0.25ms^{-1} during flood and ebb.

The currents in the channel indicate a relatively strong asymmetry with ebb currents being stronger than flood currents. The ebb period is roughly 5.5 hours compared to a flood period of about 7 hours, thus a slightly larger difference than that obtained from the tide at the Creek station (6.58 hrs vs 6.04 hrs). This can be readily seen from Fig 13 a,b, where a comparison is made between along-channel components and the sea levels at the Claudio site. The assymetry is not pronounced during neap, however. The results indicate that the sea levels lead the currents by an average of 3.45 hours (104°) and slack waters coincide with the times of high and low water. Zero velocities lag the occurrence of high water and low water by 0.6 hours and 0.2 hours respectively.

A scatter plot of east-west and north-south components indicates that both flood and ebb velocities are confined along the axis of the channel as shown in Fig 12.

3.3 Salinity Variations

We observed clear seasonal variations in salinity (see Table 5). The lowest salinities, 33 PSU were measured in the uppermost region of the creek in June while the highest values, 38 PSU were measured in September, also in the upper region of the creek. At the entrance, the variations were minor with salinities of 35 ± 0.4 PSU at high water. The salinities in the creek waters are clearly related to the periods of dominating evaporation and precipitation. During the dry season in September, evaporation in the upper part of the creek exceeds fresh-water inflow resulting in higher salinities than the oceanic. During the rainy season in June, fresh-water inflow exceeds evaporation causing lower salinity in the upper region. The salinity distribution in the creek was generally uniform throughout the depth. This indicates that the creek waters are vertically well mixed.

During a 24 hour measurement at Claudio in September 1996, we also found a clear ebb-flood salinity difference, with ebb tides having up to 1 PSU higher mean salinities compared to flood tides (Fig 17). This result indicate that we may have a sustained stratification in this part of the channel where the depths exceed 20 m. The measurements were done from a jetty, with depths of a few meters only, so we were not able to test this hypothesis.

3.4 Temperature Variations

Figs 15 a,b show time series of temperature from the tide gauge stations. The temperatures at the Claudio station varied from 24.2°C to 28.9°C with a mean of 27.2°C while those observed at the Creek station varied from 27.8°C to 30.1°C with a mean of 28.9°C.

The Creek site is characterised by higher mean temperatures, 1.7°C on the average. The lagoon is subject to more effective heating due to less evaporation loss, we believe and restricted cooling from deeper waters (which happens to the oceanic water).

In Fig 16 a,b, a comparison is made between temperatures and sea levels at the tide gauge stations. Maximum temperature for the Creek station occurs at about 1600. At Claudios it occurs two hours earlier. At both stations, the temperatures decreases during flood, but the semi-diurnal variability is much more clear at Claudio station, where the flood is bringing more cool water into the creek.

In general, the temperature variations are dominated by the diurnal solar heating and night cooling due to a combination of evaporation and long wave back radiation.

3.5 Volume fluxes driven by the tides

Calculations of mean tidal volume fluxes through the channel were based on the Creek tide gauge measurements and the creek mean surface area using the following equations;

$$Q_{fl} = \frac{A_S.h}{T_{fl}} \quad \text{and} \quad Q_{eb} = \frac{A_s.h}{T_{eb}}$$

where Q_{fl} and Q_{eb} are flood volume flux and ebb volume flux respectively. T_{fl} is the average flood duration, 6.58 h and T_{eb} is the average ebb duration, 6.04 h at the Creek station. A_S is the mean surface area of the creek including the channel inside the Claudio station. The surface area of Mtwapa creek is 13.6×10^6 m^2 at HWS but reduces to almost 20% of that value during LWS. The mean surface area $A_s \approx 8 \times 10^6$ m^2; h is the tidal range (2.8 m for spring and 0.8 m for neap).

We also estimated the mean flood velocity, Q_{fl}/A_x and mean ebb velocity, Q_{eb}/A_x. Where A_x is the cross sectional area of the channel at Claudio. This area was determined to 3375 m^2 after a 10% reduction due to contraction of the flow.

The following results were obtained;

	During spring	During neap
Mean flood volume flux	980 m^3s^{-1}	300 m^3s^{-1}
Mean ebb volume flux	1070 m^3s^{-1}	330 m^3s^{-1}
Mean flood velocity	29.1 cms^{-1}	8.8 cms^{-1}
Mean ebb velocity	31.7 cms^{-1}	9.8 cms^{-1}

The average flood and ebb velocities as observed from the current meter data were, during spring 28.7 cms^{-1} and 32.4 cms^{-1} respectively while the corresponding observations during neap tide were 9.3 cms^{-1} and 10.2 cms^{-1}. Thus, the velocity measurements compare suprisingly well with the computed values given above.

3.7 Heat flux

Encouraged by the good results from the comparison given above, the heat flux was calculated from the current meter data by using the equation

$$Q_T = \int_t \rho c_p A_x U(t) T(t) \partial t$$

where ρ is the density of sea water (1025 kgm^{-3})

c_p is the specific heat of sea water (4200 $J(kg°C)^{-1}$

A_x is the cross sectional area of the channel at Claudio (3375 m^2)

U is the current velocity, T is the water temperature and t is the duration of the observations

Thus, we computed an average advective heat flux from the lagoon to be approximately 40Wm^{-2}, which seems reasonable regarding results from radiation and sea surface heat flux computations (see eg. Mahongo, 1997).

3.7 Water exchange and residence times

To calculate water exchange between the lagoon and the ocean, we used different approaches. First we utilised the seasonal salinity observations shown in Table 5. Here, the creek data were from far upstream, and not at the Creek station. We divided between two periods; measurements from June (1), assumed to be within the rainy season, and measurements from August-September (2), assumed to be within the dry season. The following estimates were used for calculations of the water exchange (Q's in m^3s^{-1});

	Q_f	Q_r	Q_e	Q_p	dS	S_o
Per 1	0.65	0.35	-0.3(2mm/d)	0.6(4mm/d)	-1.1	34.72
Per 2	-0.9	0	-0.9	0	1.53	35.20

By using eq. (10), assuming steady state, and $dS = S_i - S_o$, period 1 gave a net volume exchange Q_o, of 20.7 m^3s^{-1} and period 2 a net volume exchange of Q_o=21.0 m^3s^{-1}. Thus, the residence time, T is approx. 12 days. These estimates are certainly overestimated, giving too low exchange rates and too long residence times as the point for observing salinities in the creek was in its upper end. The results are not representative as averages for the creek volume, and therefore we did an alternative calculation of the water exchange as described below.

According to Fig 15, there is a mean temperature difference, dT between the Creek station and the Claudio station of about 1.3°C (28.9-27.6) during the period when both instruments were deployed. It reflects an additional heat input through the creek surface, F_T, compared to the ocean (over relevant scales). A simple heat balance equation, valid for a long-term steady state may be written as $Q_{out}T_{out} = Q_{in}T_{in}+F_T/\rho C_p$, where the Q's are the long-term averages exchange flows. This expression simplifies by assuming $Q_{out} \approx Q_{in}$ implying that $Q_{out}dT=F_T/\rho C_p$. The net heat flux out of the system was calculated from the current measurements at Claudio (as shown above) to be 40 Wm^{-2}. This flux should

equal the net heat input to the creek multiplied by the creek mean surface area (A_s), so that we obtain $Q_{out}dT=40A_s/\rho C_p$. This equation gives a $Q_{out} \approx 80\ m^3s^{-1}$, thus four times larger than the value of Q obtained for the uppermost part of the creek. Q_{out} corresponds to a residence time, T of approximately 3 days. This residence time is more reasonable as an average for the creek, keeping in mind that at spring tide, almost 80% of the water is shifted during each tidal cycle, while at neap, the rate decreases to about one third of that value. Thus, the average during neap may be about 4 days while during spring the average residence time is only about 2 days.

3.8 Model results on sea levels

Fig. 19 shows a comparison between the predicted sea levels obtained by solving Eq. (5) and the observed sea levels at the Creek station. The model is forced by the sea level fluctuations at the entrance of the channel. The sum of eight tidal harmonics with amplitudes corresponding to the semi-diurnal and diurnal constituents (see Table 3) observed at the Claudio station have been used to represent the ocean forcing tide.

The model was run with different values of the friction coefficient k in order to obtain the ''best fit'' to the observed sea levels at the Creek site. The value of k that produced a reasonable fit was $1.9 \times 10^{-5}\ ms^{-1}$. As shown in Fig 19, the model gives reasonable results for both amplitudes and phase lags.

The comparison is encouraging considering the simplicity of the model. The model does not take into account, however the varying geometry of the channel and it uses the mean depth only. It also assumes that sea level variations in the channel are laterally homogeneous which makes it one dimensional model in space. To improve the model, it is necessary to take the lagoon topography into account.

The model also estimates the disipation of tidal energy during propagation. The computed rate of dissipation obtained by solving Eq. (6) is 6.19×10^3 W.

4. DISCUSSION

The tide gauge measurements were subject to harmonic analysis (Table 3). The amplitudes for the major tidal constituents at the outer station, Claudio compare well with those obtained from Mombasa (Pugh, 1979). There were differences of between 36-40° in phase lags. These differences appear because we referred the phases to the Greenwich meridian while by Pugh's data are given relative to the local meridian. In comparison with Nguli (1994) and Odido (1994) tidal data from Mombasa, the amplitudes compare fairly well for both sites. However, the phases differ because they referred the phases to the M_2 tide.

The phase lag between the Creek station and the Claudio station was found to be between 15-20 minutes. It is sensitive to levelling. Levelling of the tide gauges was made by assuming that the sea level was equal at the time of slack water in the channel. We assumed a constant air pressure and subtracted that from the original tide gauge records. This assumption introduces deviations in the absolute sea level equal to the deviations in air pressure from the average. These are small however usually less than 5mbar or ±5cm in absolute sea levels. We also did float drouges measurements indicating that there were variabilities in the time for slack water and thus it might be worthwhile to improve the way of levelling.

Our results show that the tidal range is reduced by 10-30cm in the creek. This reduction is due to frictional effects within the channel which act to dissipate the energy of the tide during propagation. The semi-diurnal components are more damped than the diurnal and long periods constituents. The reduction in tidal amplitude is a common feature observed in choked coastal systems, where the narrow channel that connects them to the ocean acts as a filter which allows longer period changes to penetrate but damps out the higher

frequencies (Kjerfve and Magill, 1989; Wijerathne *et al.*, 1995). The development of phase changes in the tide (~ 5° between the two stations for the M_2 constituent) and by amplitude decay of the total spectrum (by about 10% between the two stations) supports this conclusion. The non-linear response to tidal forcing is small as demonstrated by the low M_4/M_2 ratio.

In Fig 13a, the observed along channel velocity components are compared to the tide at the Claudio station. The assymetric velocity is a key parameter which reflects the topography (hypsographic curve) of the creek. The rapid change in velocity from the time near high tide and onwards indicates that there are large area (and volume) changes above MSL. Higher velocities during ebb (0.8 ms^{-1}) compared to flood (0.5 ms^{-1}) is because of the different flow dynamics during filling of the mangrove areas compared to during emptying (Wolanski, 1990). At some instant, when the sea level is approximately 0.5 m below MSL, the ebb velocities decreases rapidly from 0.8 ms^{-1} to about 0.2 ms^{-1}. This decrease is simultaneous with a surprising decrease in dh/dt at the Creek station (see Fig 16 b). Normally, when this appears, one would think of a sill which, when the water depth is decreasing starts to restrict the flow. In such a case however, dh/dt would continue to decrease, like it does in Bamburi lagoon just south of Mtwapa (cf Kirugara, 1997). This is not the case here, and thus we suggest that the feature is caused by baroclinic wave drag in the inlet channel. If there is stratification in the deeper part of the inlet, the high channel velocities during ebb would result in a lifting of the deeper waters to the near surface, thereby reducing the ebb velocities by building up a hydraulic control, which intermittently will result in stack up of water in the creek and in a decreased dh/dt.

The small residuals observed both at the Claudio and Creek stations indicate that meteorological forcing due to windstress or fluctuations in air pressure plays a minor role in the creek-ocean exchange processes. In this case it also indicates that water exchange in the creek is exclusively caused by tidal forcing.

Although there is very little asymmetry in the tide, the current measurements in the channel (Fig 13a) reveal an asymmetry of ebb-dominance, i.e high ebb velocities and shorter ebb periods. This asymmetry of ebb-dominance fits well with the conclusions concerning topography by Shetye and Gouveia (1992); Mtwapa creek is a deep tidal channel surrounded by mudflats. The features are similar to those in Hinchinbrook channel (Wolanski *et al.,* 1980) and in the North inlet which is a channel surrounded by salt marshes (Kjerfve *et al.*, 1991). Ebb-dominance has also been observed in deep sub-tidal channels with mudflats eg. the Wachapreague inlet (Boon and Byrne, 1981). Non-linear friction effects in mangrove swamps could result in an asymmetry between the filling and emptying of the mangrove swamps (Wolanski *et al.*, 1980).

Salinity measurements were made in the upper region of the creek. These were used to estimate water exchange including a residence time of 12 days. This high value is representative only for the waters in the upstream part of the creek. As an alternative we also used heat flux and temperature measurements to calculate the residence time. That calculation gave a residence time of 3 days which is valid for the average volume, and much more reasonable considering that almost 80% of water is exchanged during each tidal cycle during spring.

The discharge from Mto mkuu river is seasonal and very low. The effect of fresh water inflow is experienced only far upstream and only on the salinity. Salinity measurements upstream reflect this effect during the month of June when salinities were about 34 PSU (Table 5). For the rest of the measuring period, salinities were higher inside as compared to the ocean due to evaporation. The higher salinities during ebb as compared to flood observed at Claudio in September supports this conclusion. The peak fresh water discharge (0.7 m^3s^{-1}) is very small as compared to tidal volume flux (300-1000 m^3s^{-1}).

This indicates that water exchange between Mtwapa creek and the ocean is caused by tides, exclusively.

From the results of the model, the value of friction coefficient k, is 1.9×10^{-5} ms^{-1}. This value is of the same order with values obtained using linear friction law in shallow, narrow tidal channels. Bennett (1975) observed a value of $1.8 \times 10^{-5} ms^{-1}$ based on an analytical model in the Bristol channel. Shetye and Gouveia (1992), also using an analytical model and linearised friction obtained a k value of 1.6×10^{-5} ms^{-1} for the Fleet. Pugh (1979) observed values between 0.015 ms^{-1} and 0.024 ms^{-1} which are substantially higher than ours in spite of having used the same formula. The difference is due to the effect of uneven coral bottom and high velocities (up to 3 ms^{-1} on spring tides) increasing friction in the atoll channel.

5. CONCLUSIONS

The tides in Mtwapa creek are typically semi-diurnal with spring tidal range of 3.10m at the entrance and 2.81m inside. The corresponding neap tidal range is 0.93m and 0.80m respectively. The sea level variations are exclusively caused by the tidal action. Within the creek, the flood tide lasts for 6.58 hours while ebb lasts for 6.04 hours.

Ebb currents are stronger than flood currents. This classifies Mtwapa creek as a weakly choked lagoon, with an assymetry of ebb-dominance.

The mean tidal volume flux of water calculated from sea level observations is 1000 m^3s^{-1} during spring and 300 m^3s^{-1} during neap. The mean tidal velocity during spring is 30 cms^{-1}

and during neap is 10 cms^{-1}. Maximum ebb and flood velocities are 0.8 ms^{-1} and 0.5 ms^{-1} respectively.

The residence time for the creek waters is of the order of 3 days but varies with neap and spring. In the upper end we found a residence time of 12 days. Fresh water discharge is very small as compared to the tidal volume fluxes.

The temperature variations are diurnal with maximum temperatures occuring at 1600 within the creek. They are sligthly sensitive to the semi-diurnal variations caused by the tide.

The advective heat flux through the channel based on three days of currents and temperature observations is 40 Wm^{-2} indicating a corresponding net heating through the sea surface. The rate of tidal energy dissipation in Mtwapa creek during propagation in one cycle of M_2 is 6.2×10^3 W.

This study of water exchange is the first to be carried out in Mtwapa creek. In future studies, it will be necessary to use air pressure to correct the pressure gauge data. It will also be necessary to measure currents for longer duration (at least two weeks) in order to perform harmonic analysis. Salinity measurements should be conducted to cover the two monsoon seasons. The most important issues, however concerns a better topographic mapping and better input data on the net fresh-water balance.

ACKNOWLEDGEMENTS

This work was funded by the Swedish Agency for Research Cooperation with developing countries (SAREC) through the Department of Oceanography, University of Gothenburg. I wish to thank Dr. Lars Rydberg and Ulf Cederlöf for the lectures, field work support and guidance they provided during the writing of this thesis. I also wish to express my appreciation to Drs. Ezekiel Okemwa, the director of Kenya Marine and Fisheries Research Institute (KMFRI) and Olof Linden for their administrative support.

My thanks also goes to Dr. Nyawira Muthiga of the Kenya Wildlife Services (KWS) for her support through provision of KWS boats during field work, my colleagues Mika Odido, Michael Nguli, and Johnson Kitheka for their assistance and encouragement.

My special thanks go the the staff of KMFRI, Mariara, Kilonzo and Gaya for field work support, Mr. Ogallo for map drawings.

REFERENCES

Aubrey D.G. and Speer P.E. (1985), A study of Non Linear Tidal Propagation in Shallow Inlet / Estuarine Systems. *Estuarine, Coastal and Shelf Science* 21, 188-224.

Bennett A.F.(1975), Tides in the Bristol Channel. *Geophysical Journal of the Royal Astronomical Society* 40, 37-43.

Boon J.D. and Byran R.J. (1981), On basin hypsometry and the Morphodynamic response of coastal inlet system. Marine Geology 40, 27-48.

Boon J.D. (1975), Tidal Discharge Asymmetry in a Salt Marsh Drainage System. *Limnology and Oceanography* 20, 71-79.

Brown W.S and Trask R.P. (1980), A Study of Tidal Energy Dissipation and Bottom Stress in an Estuary. *Journal of Physical Oceanography* 10, 1742-1754.

Cederlöf U. (1995) , Msc Lecture notes on Fluid Dynamics.

Dronkers, J.J. (1964), Tidal Computations in Rivers and Coastal Waters, North Holland. New York, 518 pp.

Duing W. and Schott F. (1977), Measurements in the Source Region of the Somali Current during the Monsoon Reversal. *Journal of Physical Oceanography* 8, 278-289.

Godin G. (1988), *Tides.* Centre for Scientific Research and Education, Ensenada, Mexico, 290pp.

Heath R.A. (1981), Tidal Energy Loss in Coastal Embayments. *Estuarine, Coastal and Shelf Science* 12, 279-290.

Hill A.E. (1994), Fortnightly Tides in a Lagoon with Variable Choking. *Estuarine, Coastal and Shelf Science* 38, 423-434.

Kirugara D. (1997), Wave-Induced Net Circulation in Bamburi Reef Lagoon, Kenya. *Msc Thesis, University of Gothenburg.*

Kjerfve B., Magill K.E., Ward L.G. and Ashley G.M. (1989), Geographic and Hydrodynamic Characteristics of Shallow Coastal Lagoons. *Marine Geology* 88, 187-199.

Kjerfve B., Mirando L.B. and Wolanski E. (1991), Modelling Water Circulation in an Estuary and Intertidal Salt Marsh System. *Netherlands Journal of sea Research* 28(3), 141-147.

Kjerfve B. and Knoppers B. (1991) Tidal Choking in a Coastal Lagoon. *Tidal Hydrodynamics*, John Wiley & Sons, New York, 169-179.

Nguli M.M. (1994), Water Exchange and Bottom Friction in a Tidal Estuary. *Msc Thesis University of Gothenburg.*

Norconsult M.S. (1975), Mombasa Water Pollution and Sewage Disposal Study, vol IV.

Mahongo S.B. (1997), Radiative, Turbulent and Advective Heat Exchange in a Tidal, Shallow Tropical Lagoon: Chwaka Bay, Zanzibar. *Msc Thesis, University of Gothenburg.*

Odido M. O. (1994), Tidal Dynamics of the Tudor Creek, Mombasa, Kenya. *Msc Thesis, University of Gothenburg.*

Parker B.B. (1984), Frictional Effects on the Tidal Dynamics of a Shallow Estuary. *Tidal Hydrodynamics* pp 237-268.

Pugh D. (1979), Sea Levels at Aldabra Atoll, Mombasa and Mahe, Western equatorial Indian Ocean, related to tides, meteorology and ocean circulation. *Deep-Sea Research* 26A, 237-258.

Robinson I.S. Warren L. and Longbottom J.F., (1983), Sea-Level Fluctuations in the Fleet, an English Tidal Lagoon. *Estuarine, Coastal and Shelf Science* 16, 651-668.

Rydberg L. and Wickbom L. (1996), Studies of Tidal Choking and Bed Friction in Negombo Lagoon, Sri Lanka. *Estuaries* 19, 540-547.

Shetye S.R. and Gouveia A.D. (1992), On the Role of Geometry of Cross-Section in Generating Flood-Dominance in Shallow Estuaries. *Estuarine, Coastal and Shelf Science* 35, 113-126.

Smith N.P. (1985), The Decomposition and Simulation of Longitudinal Circulation in a Coastal Lagoon.. *Estuarine, Coastal and Shelf Science* 21, 623-632.

Stigebrandt (1980), Some Aspects of Tidal Interaction with Fjord Constrictions. *Estuarine, Coastal and Shelf Science* 11, 151-166.

Swift M.R. and Brown W.S. (1983), Distribution of Bottom Stress and Tidal Energy Dissipation in a Well Mixed Estuary. *Estuarine, Coastal and Shelf Science* 17, 297-317.

Wijerathne E.M.S., Cederlöf U., Rydberg L. and Arulananthan K. (1995),The Tidal Response of Puttalam Lagoon, Sri Lanka. *Ambio* 24, 444-447.

Wolanski E., Jones M. and Bunt J.S. (1980), Hydrodynamics of a Tidal creek-Mangrove Swamp System. *Australian Journal of Marine and Freshwater Research* 31, 431-450.

Wolanski E., Mazda B.K. and Gay S. (1990), Dynamics, Flushing and Trapping in Hinchinbrook channel. *Estuarine, Coastal and Shelf Science* 31, 550-580.

TABLES

Table 1. Principal harmonic constituents

Semi diurnal

Name	Symbol	Period
Principal Lunar	M_2	12.42
Principal Solar	S_2	12.00
Larger Lunar elliptic	N_2	12.66
Luni-Solar semi-diurnal	K_2	11.97

Shallow water tides

Symbol	Period
$2SM_2$	11.61
M_4	6.21
MS_4	6.10
S_4	6.00
M_6	4.14
$2MS_6$	4.09

Diurnal

Luni-Solar diurnal	K_1	23.93
Principal Lunar diurnal	O_1	25.82
Principal Solar diurnal	P_1	24.07

Long Period

Lunar fortnightly	M_f	327.87

Table 2. Classification of tides according to F-ratio

Species	F value
Semi diurnal	$0 < F > 0.25$
Mixed, Mainly Semi-diurnal	$0.25 < F > 1.5$
Mixed, Mainly diurnal	$1.5 < F > 3.0$
Diurnal	$F > 3.0$

Table 3.

Tidal Component	Claudio Amplitude (m)	Claudio Phase (°G)	Creek Amplitude (m)	Creek Phase (°G)	Mombasa Amplitude (m)	Mombasa Phase (°G)
M_2	1.007	64	0.904	69	1.055	27
K_1	0.230	36	0.228	18	0.191	356
S_2	0.543	107	0.504	93	0.521	66
O_1	0.115	39	0.089	52	0.113	0
P_1	0.053	52	0.119	84	0.055	354
N_2	0.233	52	0.186	63	0.201	6
M_f	0.063	83	0.051	122	-	-
K_2	0.145	119	0.132	87	0.139	65
$2SM_2$	0.002	7	0.005	344	-	-
M_4	0.006	197	0.031	182	0.012	137
MS_4	0.003	295	0.025	232	0.004	191
S_4	0.005	221	0.011	283	-	-
M_6	0.001	118	0.014	208	0.011	140
$2MS_6$	0.004	198	0.020	263	-	-

Table 4.

Parameter	Formula	Claudio	Creek
Form Number	$(K_1+O_1)/(M_2+S_2)$	0.22	0.21
Inequality Phase Relationship	$M_0°-(K_1°+O_1°)$	-11°	-2°
Phase Age	$0.98(S_2°-M_2°)$	42	24
Mean Range	$2.2(M_2)$	2.01	1.81
Spring Range	$2.0(M_2+S_2)$	3.10	2.81
Neap Range	$2.0(M_2-S_2)$	0.93	0.80
Tropic Range	$2.0(K_1+O_1)$	0.69	0.63
Equatorial Range	$2.0(K_1-O_1)$	0.23	0.28
Diurnal Age	$0.91(K_1°-O_1°)$	-3.2°	-31°

Table 5.

SALINITY (PSU)			
DATE	CLAUDIO	BRIDGE	CREEK
8/6/96	34.61	34.68	33.42
23/6/96	34.93	34.84	33.87
9/7/96	34.98	34.96	34.90
21/7/96	34.70	34.74	34.06
3/8/96	35.01	35.26	36.02
9/8/96	34.79	34.72	35.91
8/9/96	34.93	34.98	36.17
25/9/96	35.07	35.26	37.82

FIGURE LEGENDS

Fig 1. Map of Mtwapa Creek showing the sampling stations.

Fig 2. Bathymetry map of Mtwapa Channel.
The width has been exaggerated by a factor of 2.

Fig 3. Geological map of Mombasa - Mtwapa area, from Walters and Linton (1973).

Fig 4. (a) Monthly rainfall at Mtwapa, January-December 1995
(From Kenya Meteorological Services records);
(b) Monthly mean discharge of Mto Mkuu river (from Norconsult, 1975).

Fig 5. Sea level time series at: (a) Claudio station,January - February 1997 and
(b) Creek station, January 1997.

Fig 6. Observed sea levels at Claudio (__) and Creek (...) stations during
(a) spring tide and (b) neap tide.

Fig 7. Time series of (a) observed, (b) computed and (c) residual sea levels at
Claudio station.

Fig 8. Time series of (a) observed, (b) computed and (c) residual sea levels at
Creek station.

Fig 9. Relative energy density spectrum from sea levels at: (a) Claudio and (b)
Creek station.

Fig 10. Time series of current velocities at Claudio during: (a) neap tide,18-20
January 1997 and (b) spring tide, 7-10 February 1997.

Fig 11. Current velocities versus directions at Claudio.

Fig 12. Scatter plot of North-South and East-West current components.

Fig 13. Comparison of sea levels (__) and current velocities (...) at Claudio during:
(a) spring tide and (b) neap tide.

Fig 14. Hypsographic curve of Mtwapa creek showing; (a) surface area as function
of sea level and (b) volume of water contained within the creek as a
function of sea level.

Fig 15. Time series of temperature recorded at: (a) Claudio, January 1997
and (b) Creek, January 1997.

Fig 16. Comparison of sea levels and water temperatures at: (a) Claudio station and
(b) Creek station from 10 January 1997 at 0000 hrs.

Fig 17. Hourly salinity variations at Claudio in comparison with sea levels,
29 September 1996.

Fig 18. Sketch of a lagoon connected to the ocean by a long narrow channel.

Fig 19. Comparison of observed (__) and predicted (....) sea levels at the Creek
station.

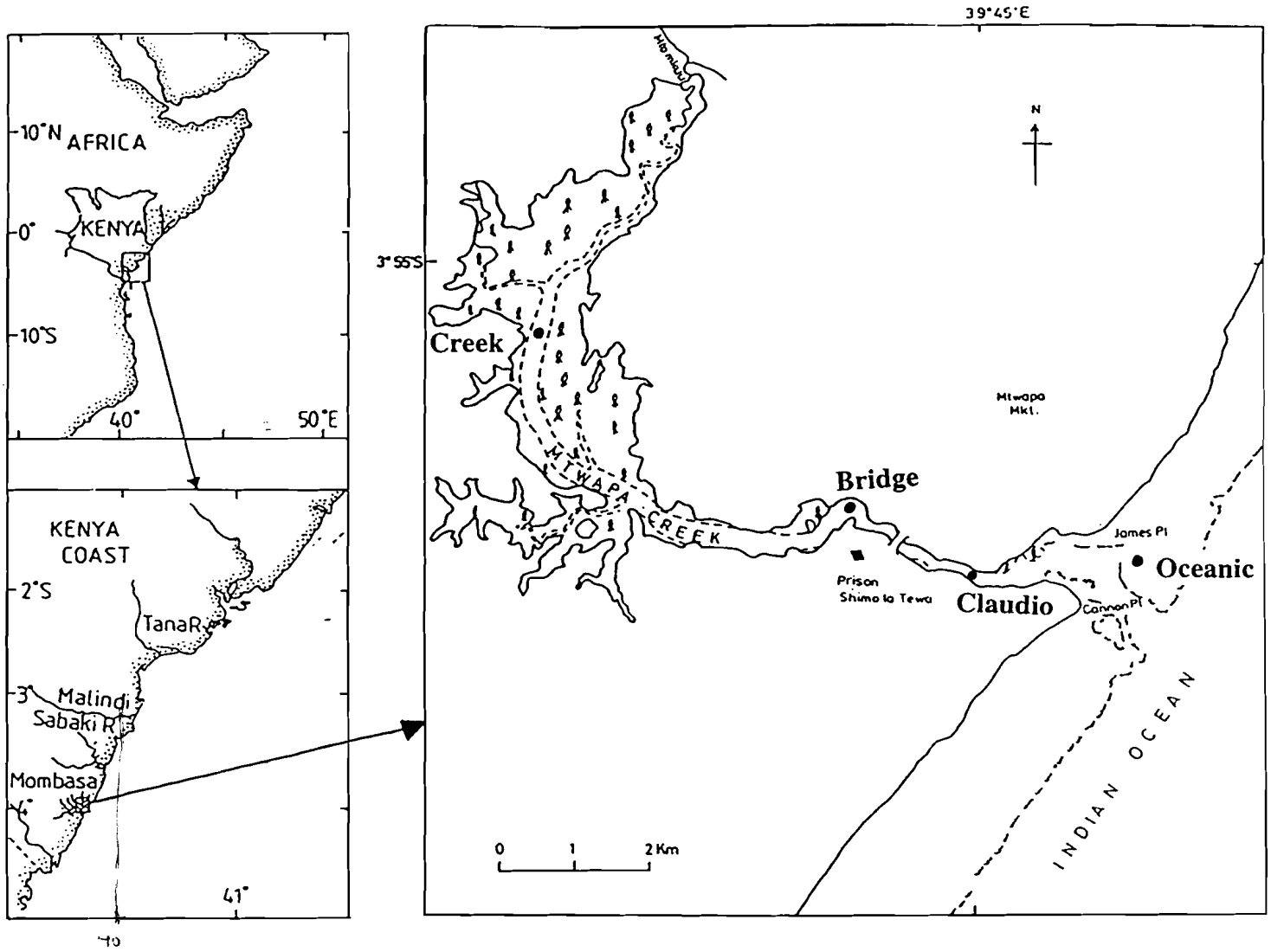

Fig 1. Map of Mtwapa Creek showing the sampling stations (•)

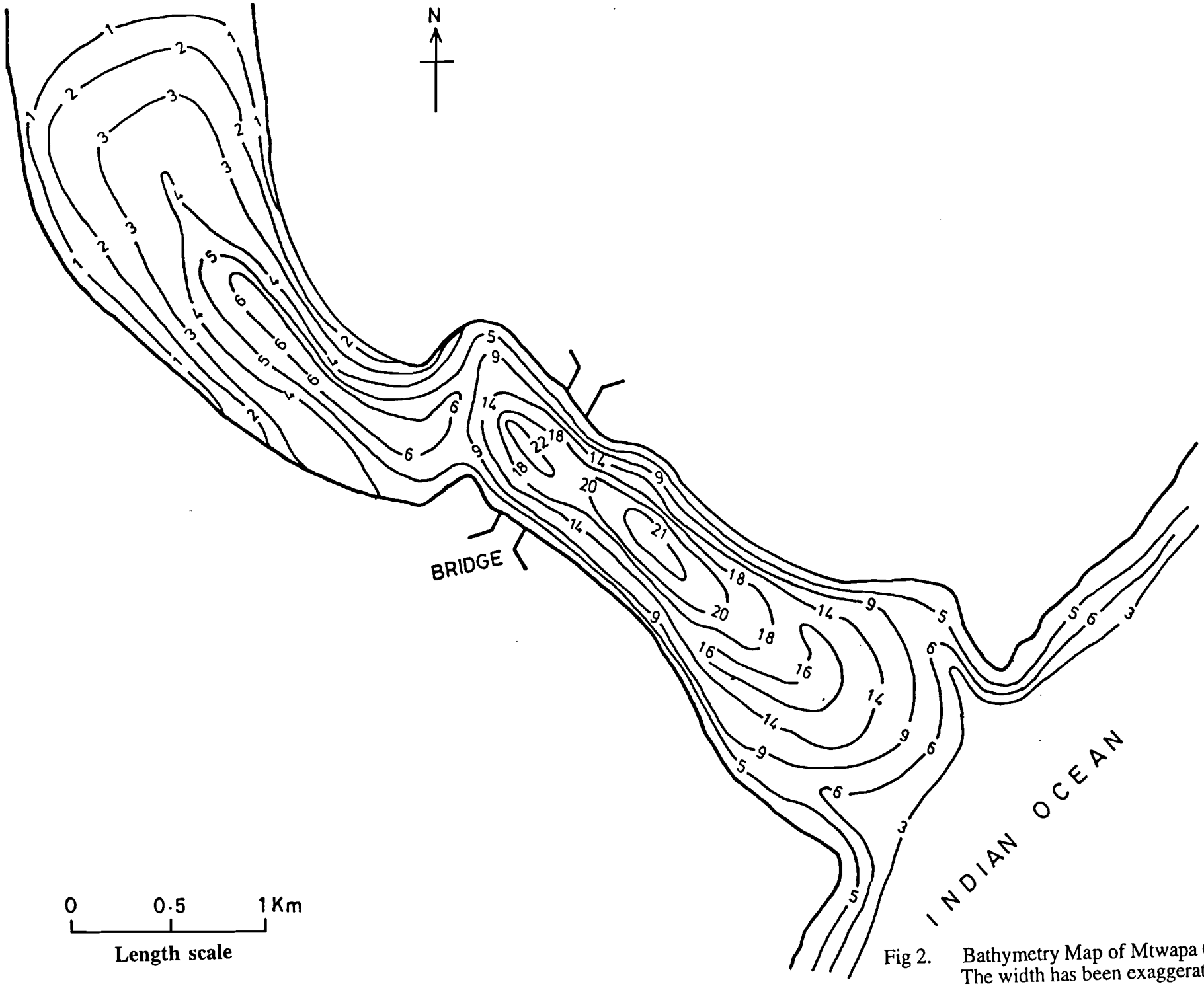

Fig 2. Bathymetry Map of Mtwapa Channel.
The width has been exaggerated by a factor of 2.

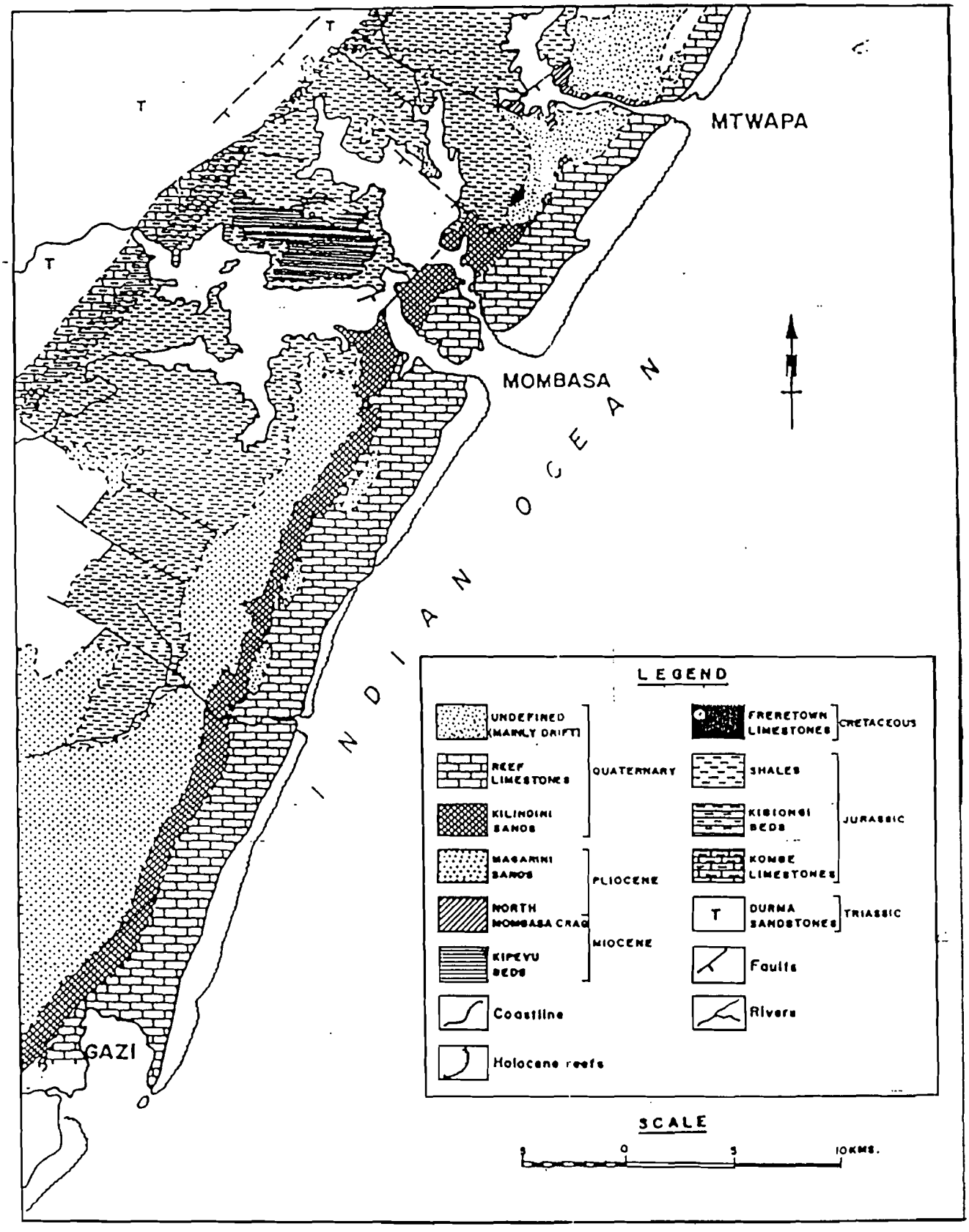

Fig 3. Geological Map of Mombasa - Mtwapa area.

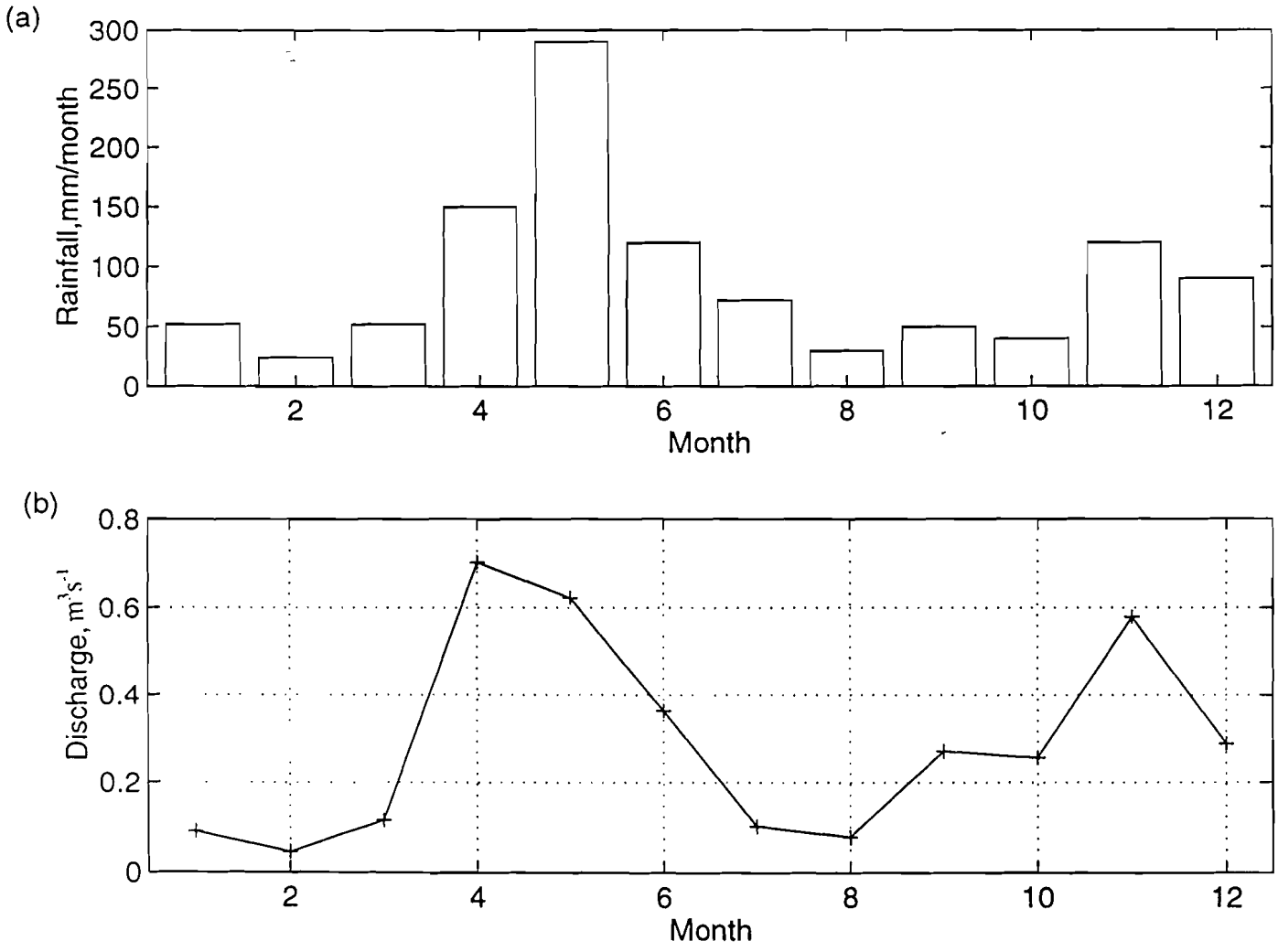

Fig 4. (a) Monthly rainfall at Mtwapa, January-December 1995
(From Kenya Meteorological Services records)
(b) Monthly mean discharge of Mto Mkuu river, from Norconsult,1975

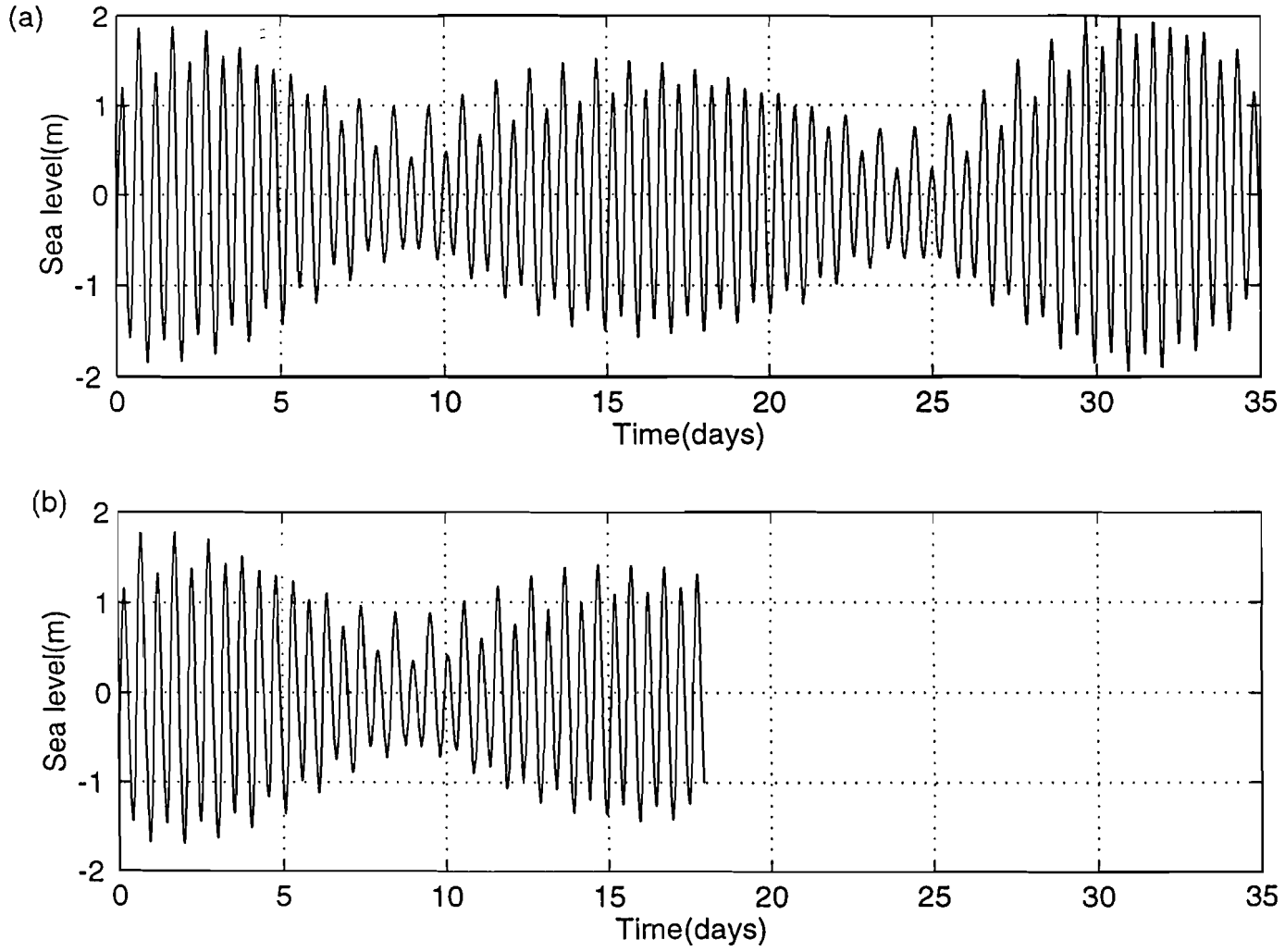

Fig 5. Time series of sea level variations at: (a) Claudio, 9 January-14 February 1997 and (b) 9 -27 January 1997; Starting time: 12:30 hrs.

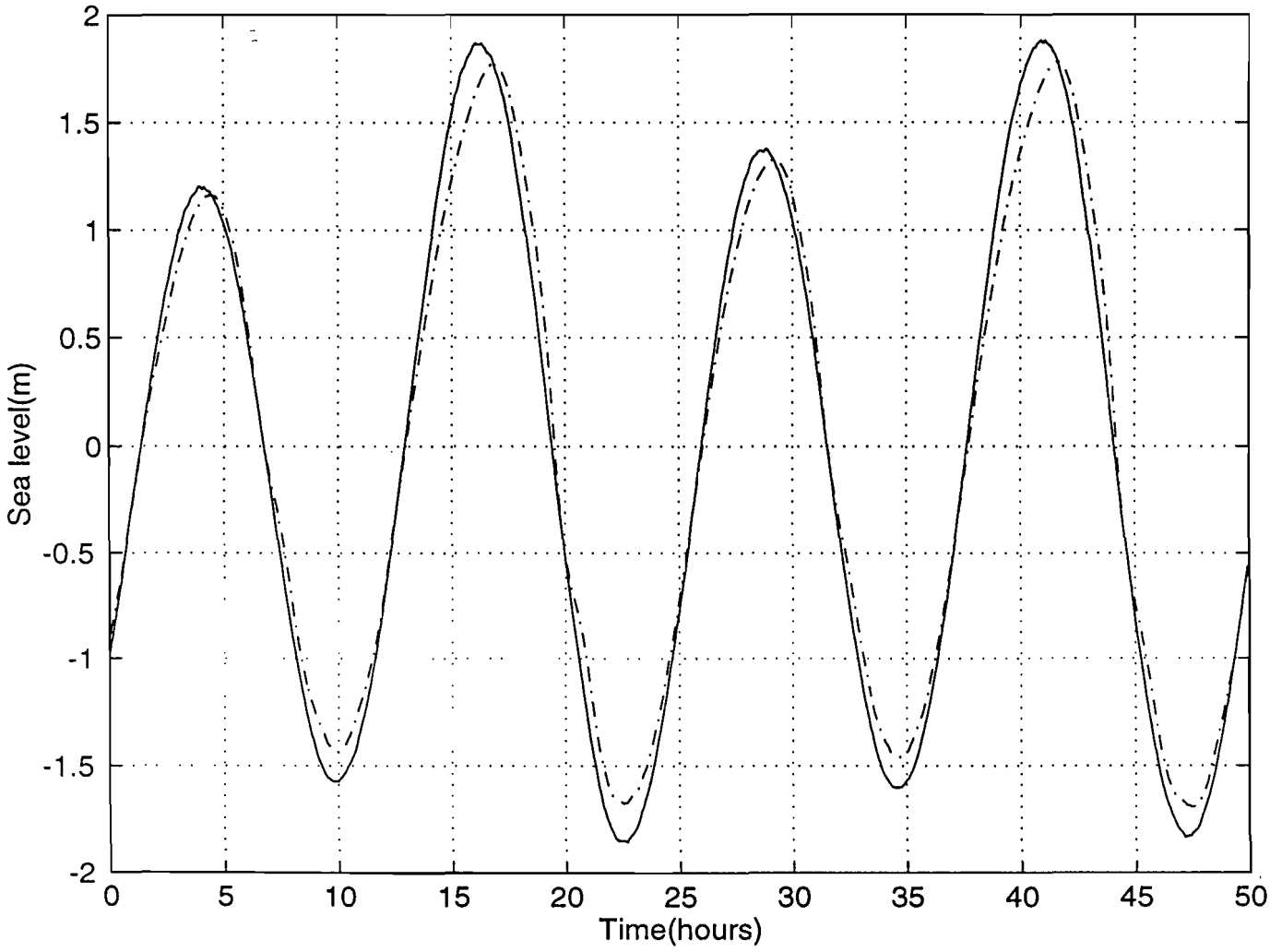

Fig 6a. Observed sea levels at Claudio (__) and Creek (...) stations during spring tide. Start time- 11 January 1997, 1300 hrs.

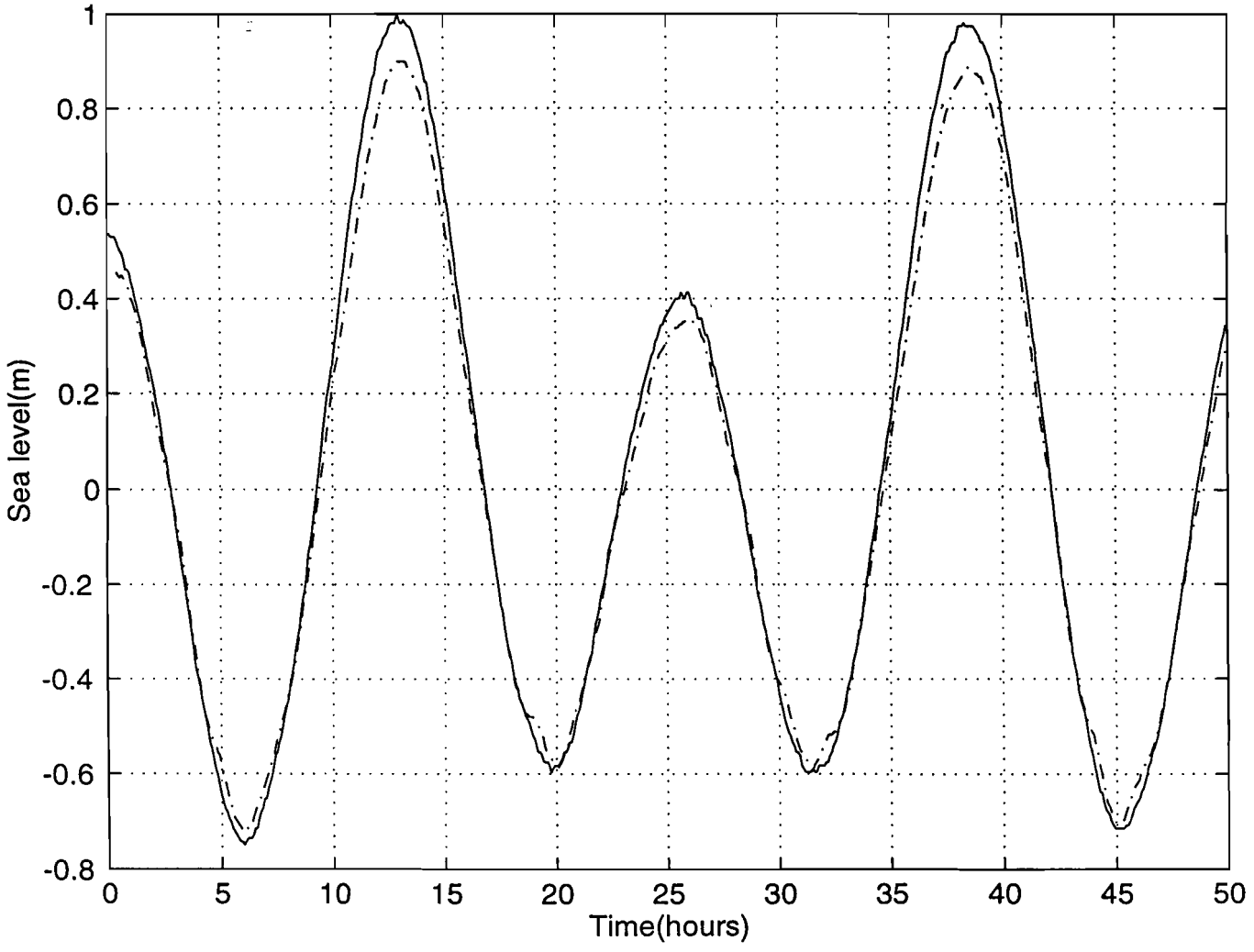

Fig 6b. Observed sea levels at Claudio (__) and Creek (...) stations during neap tide.
Start time- 17 January 1997, 0600 hrs.

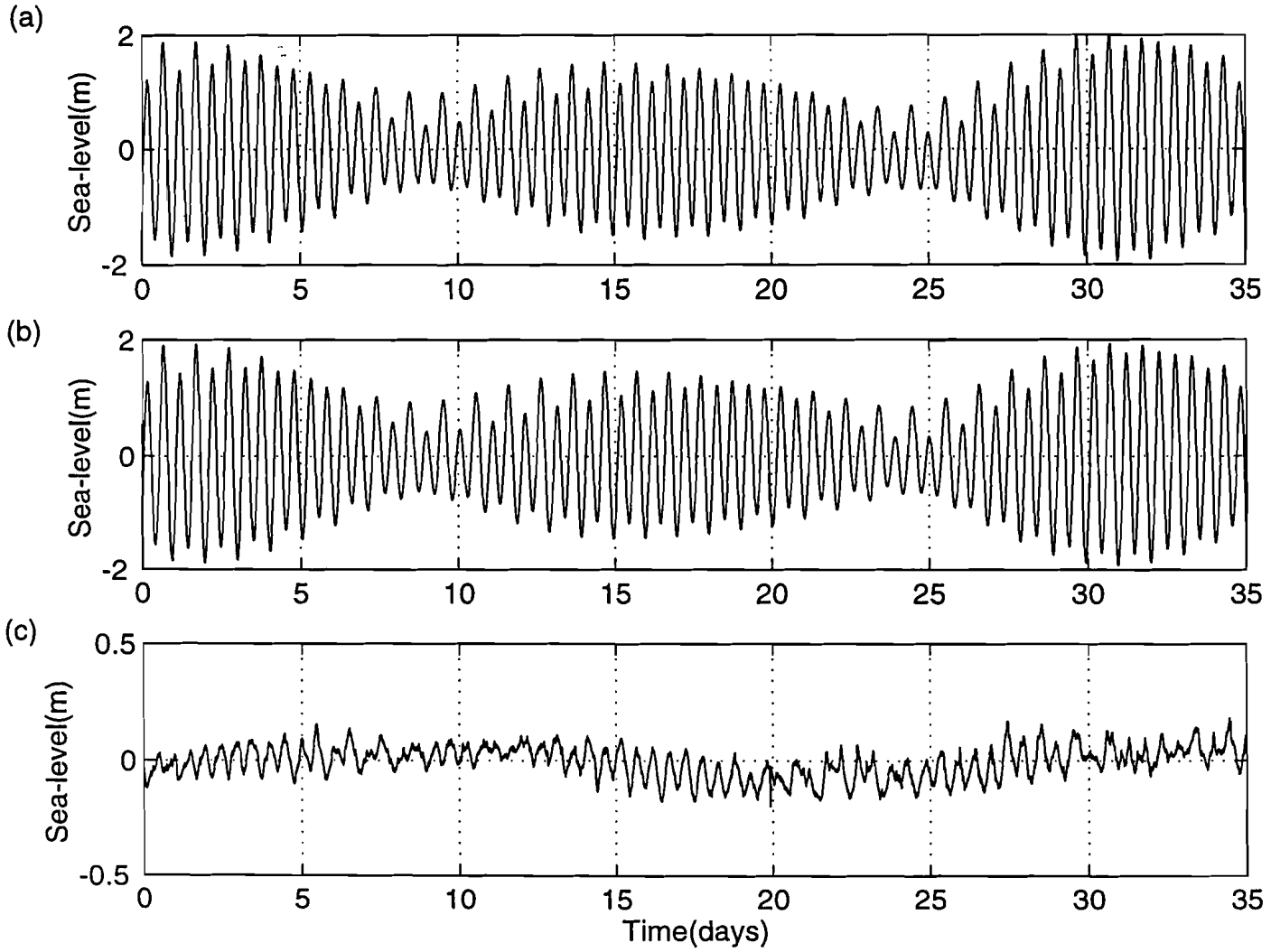

Fig 7. Time series of (a) Observed, (b) Computed and (c) Residual sea levels at Claudio station. 9 January-14 February 1997

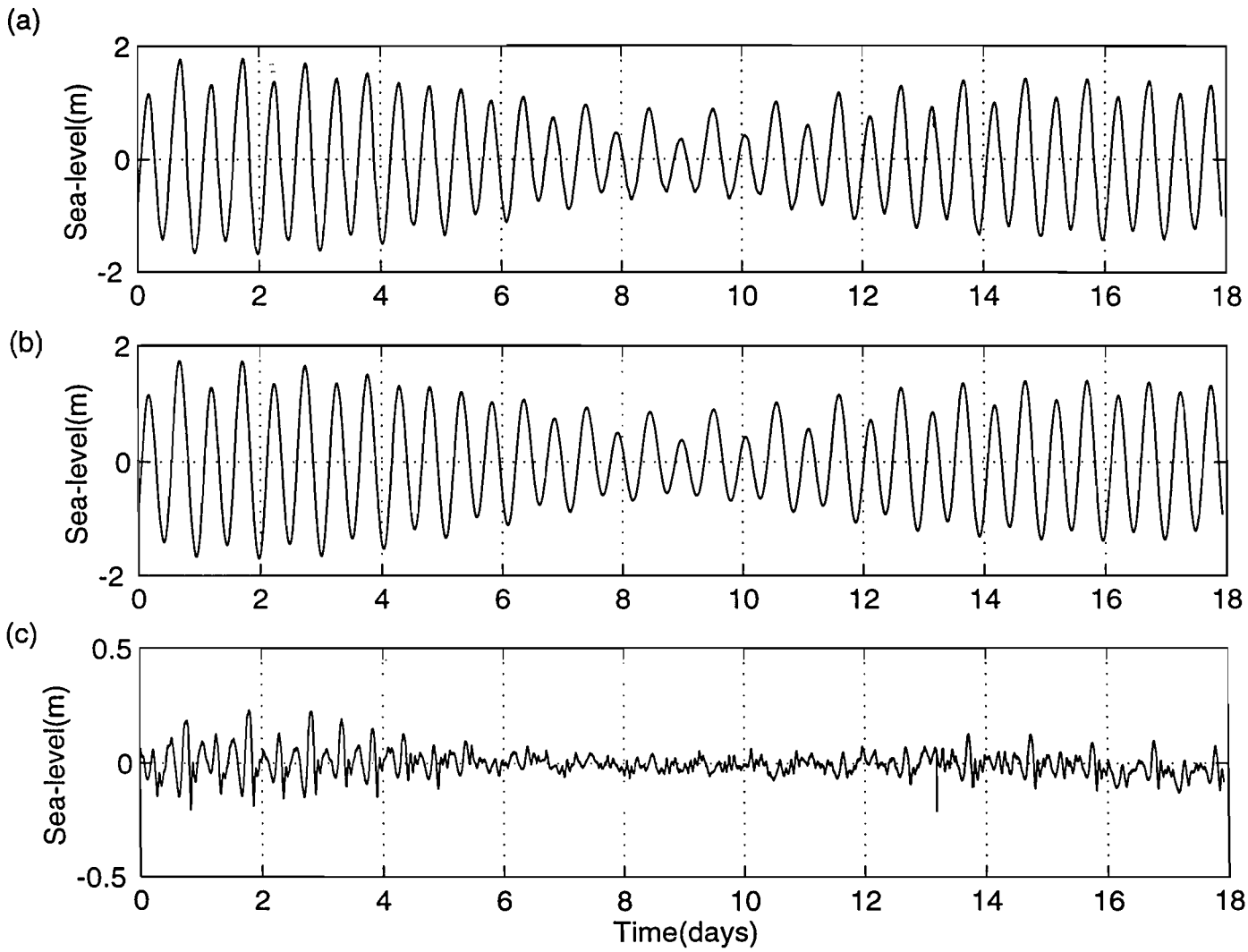

Fig 8. Time series of (a) Observed, (b) Computed and (c) Residual sea levels at Creek station. 9-27 January 1997

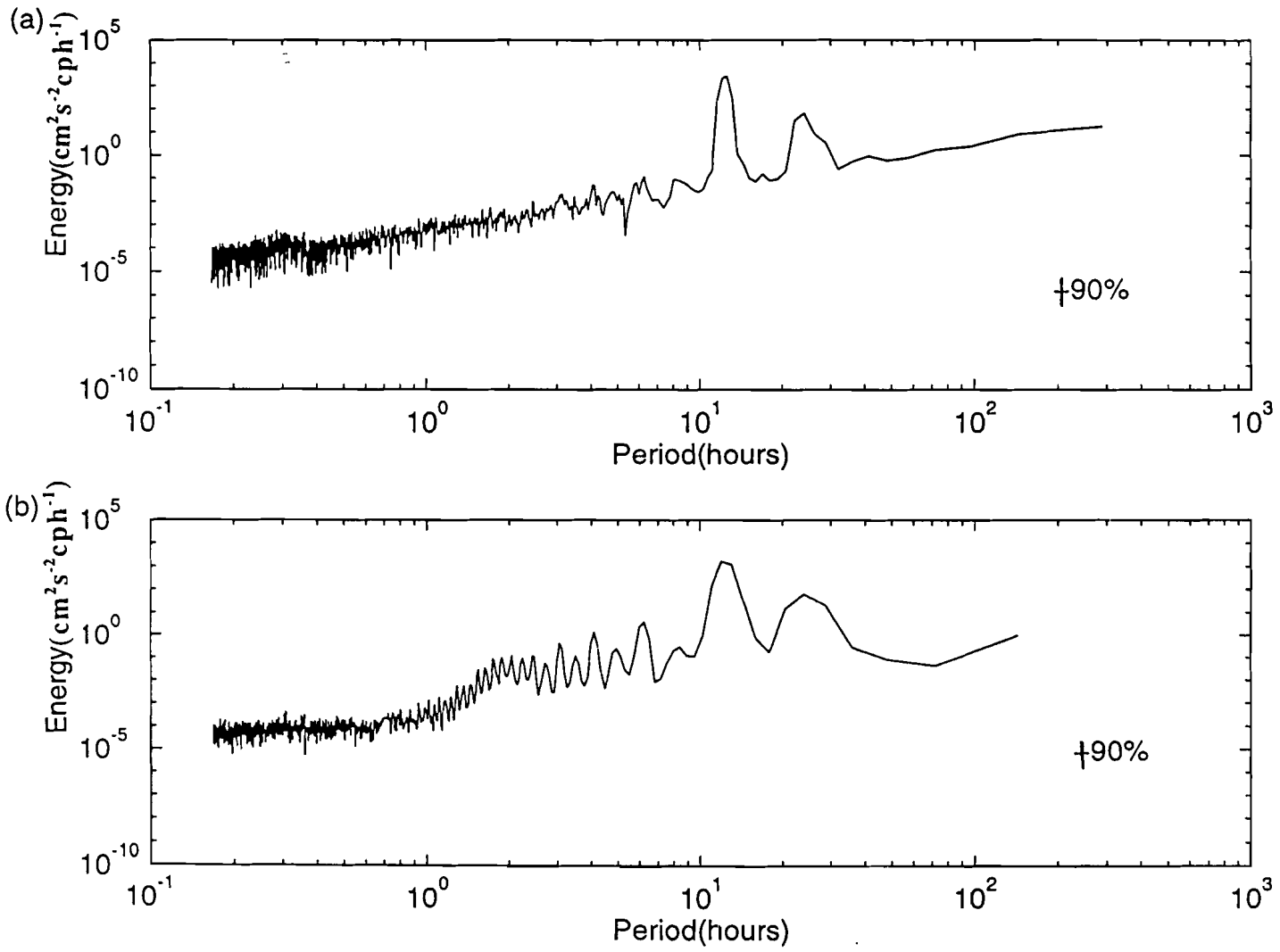

Fig 9 Relative energy density spectrum of sea levels at (a) Claudio and (b) Creek station.

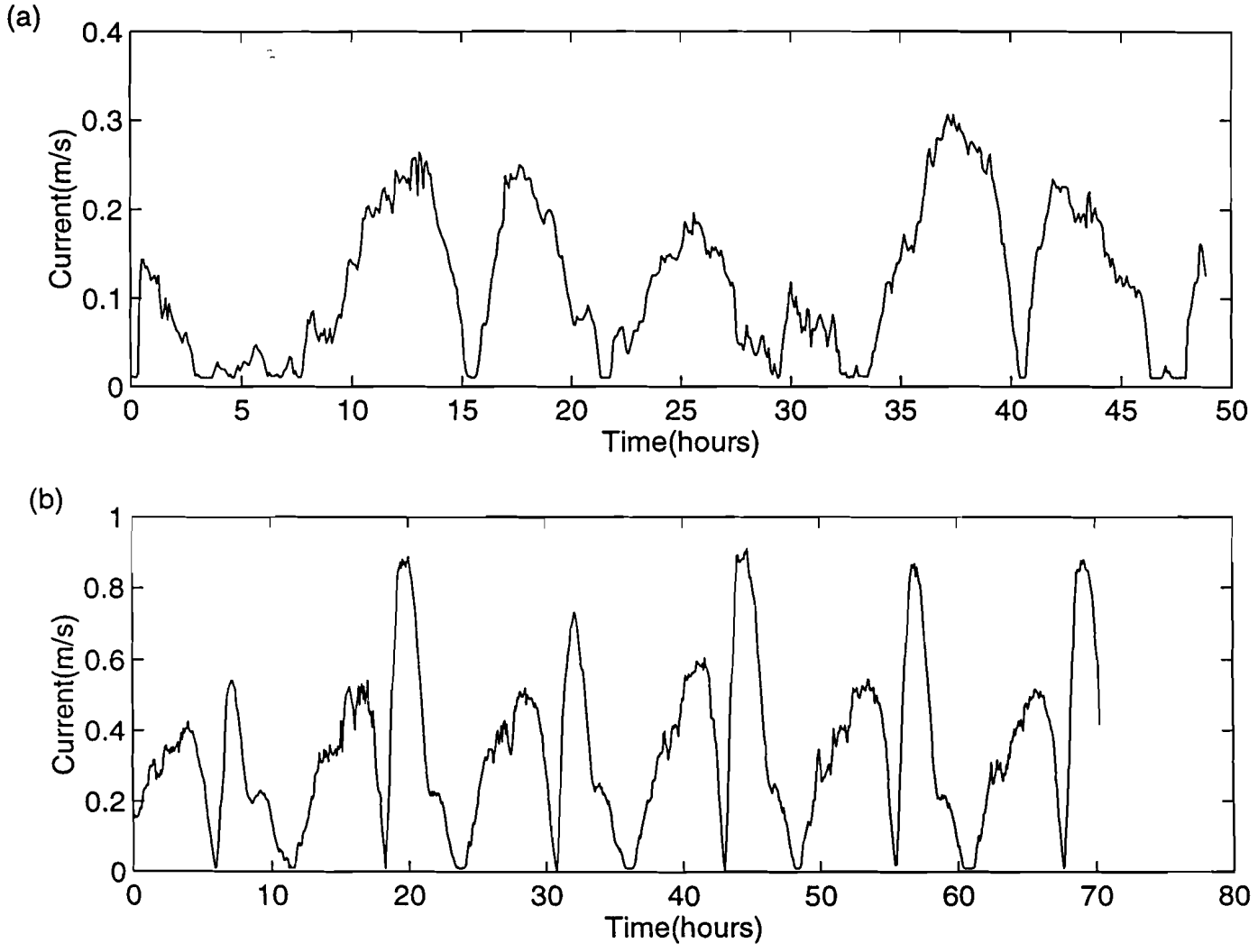

Fig 10. Time series of current velocities at Claudio during: (a) Neap tide, start time- 18 January 1997, 1000hrs ; (b) Spring tide, start time- 7 February 1997, 1100hrs.

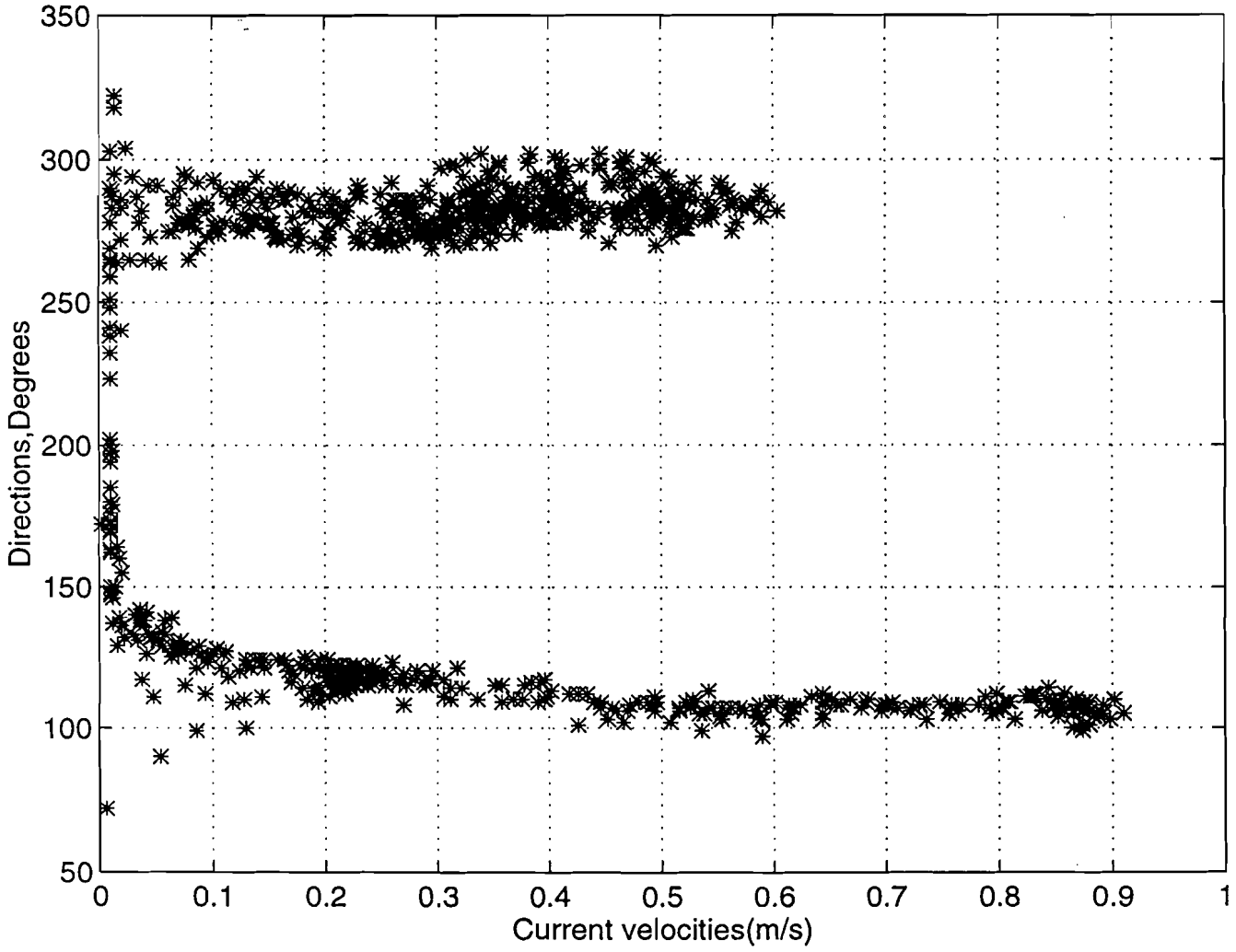

Fig 11. Current velocities versus directions at Claudio.

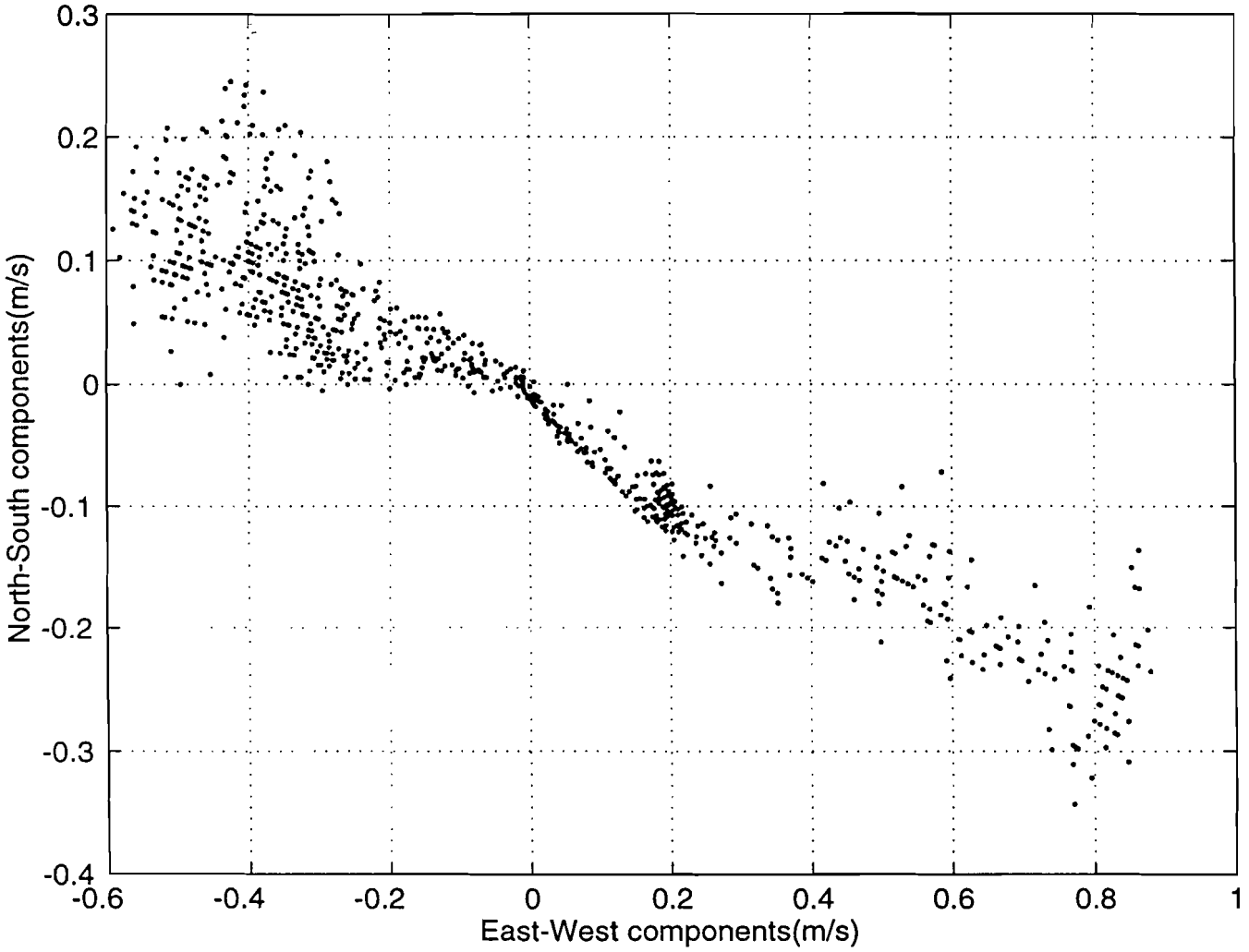

Fig 12. Scatter plot of North-South and East-West current components at Claudio during spring tide, 7-10 February 1997.

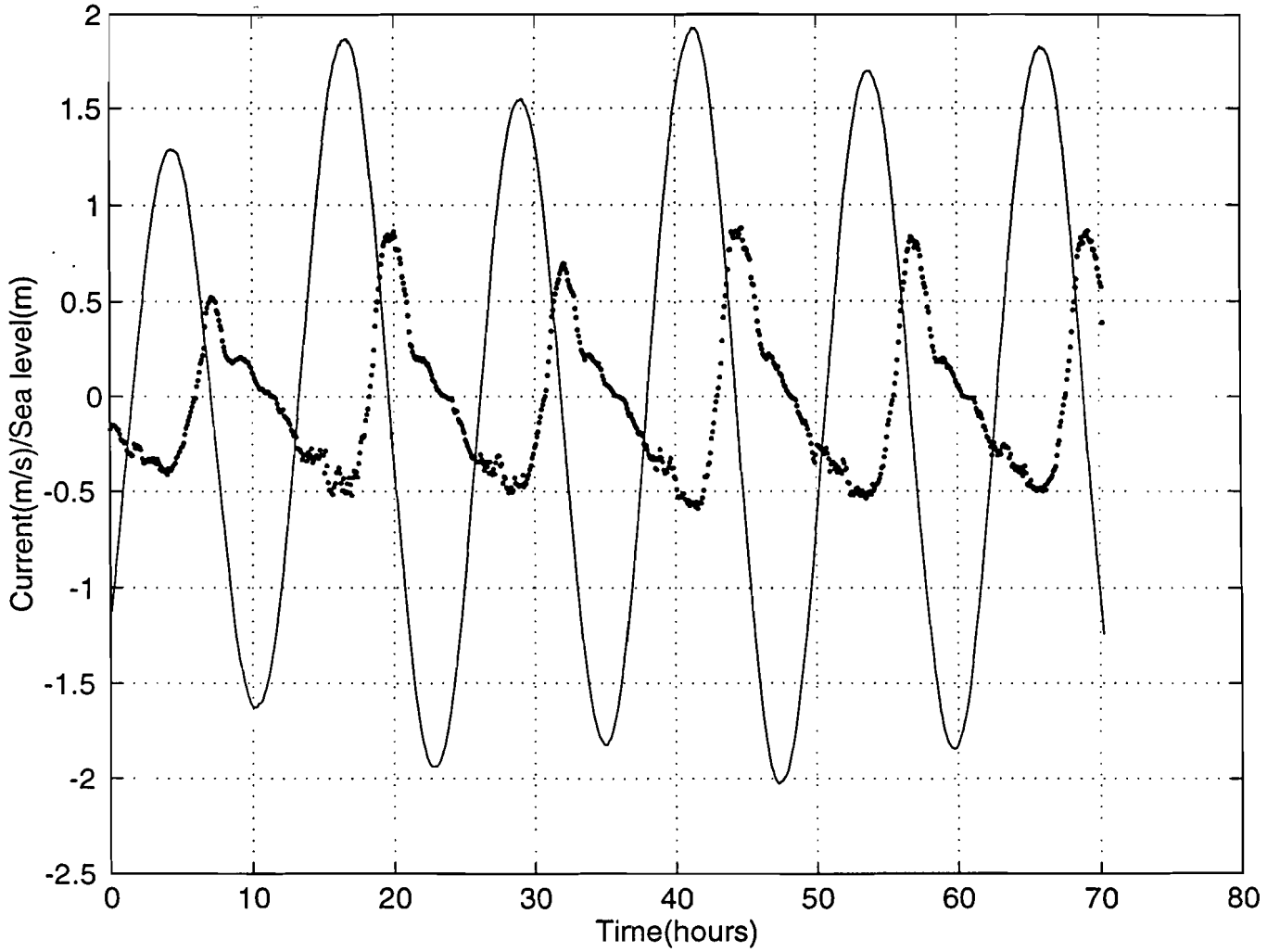

Fig 13a. Comparison of sea levels (__) and along-channel velocities (...) at Claudio during spring tide; start time - 7 February 1997, 1100hrs.

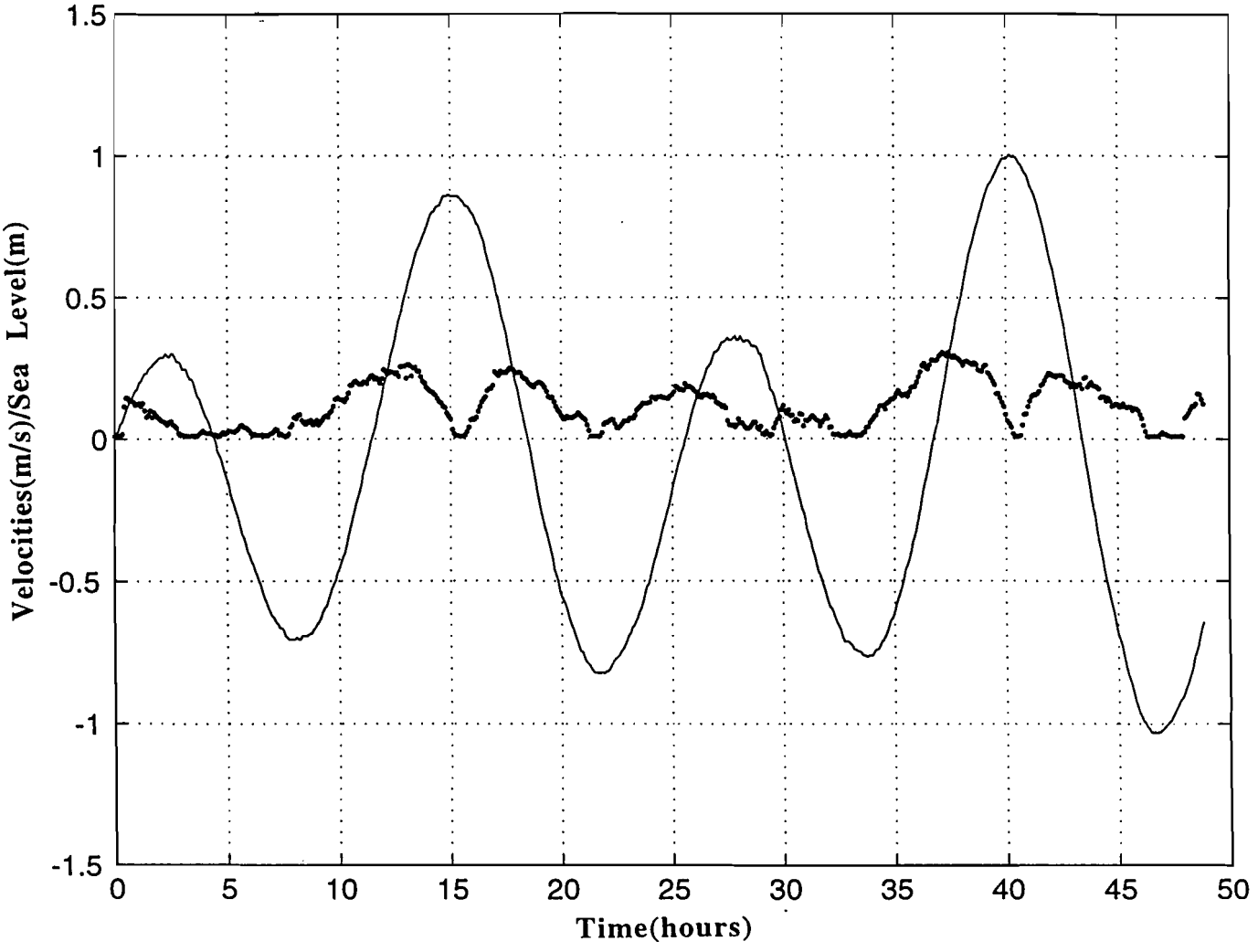

Fig 13b. Comparison of sea levels (__) and velocities (magnitude) (...) at Claudio during neap tide; start time- 18 January 1997, 1000hrs.

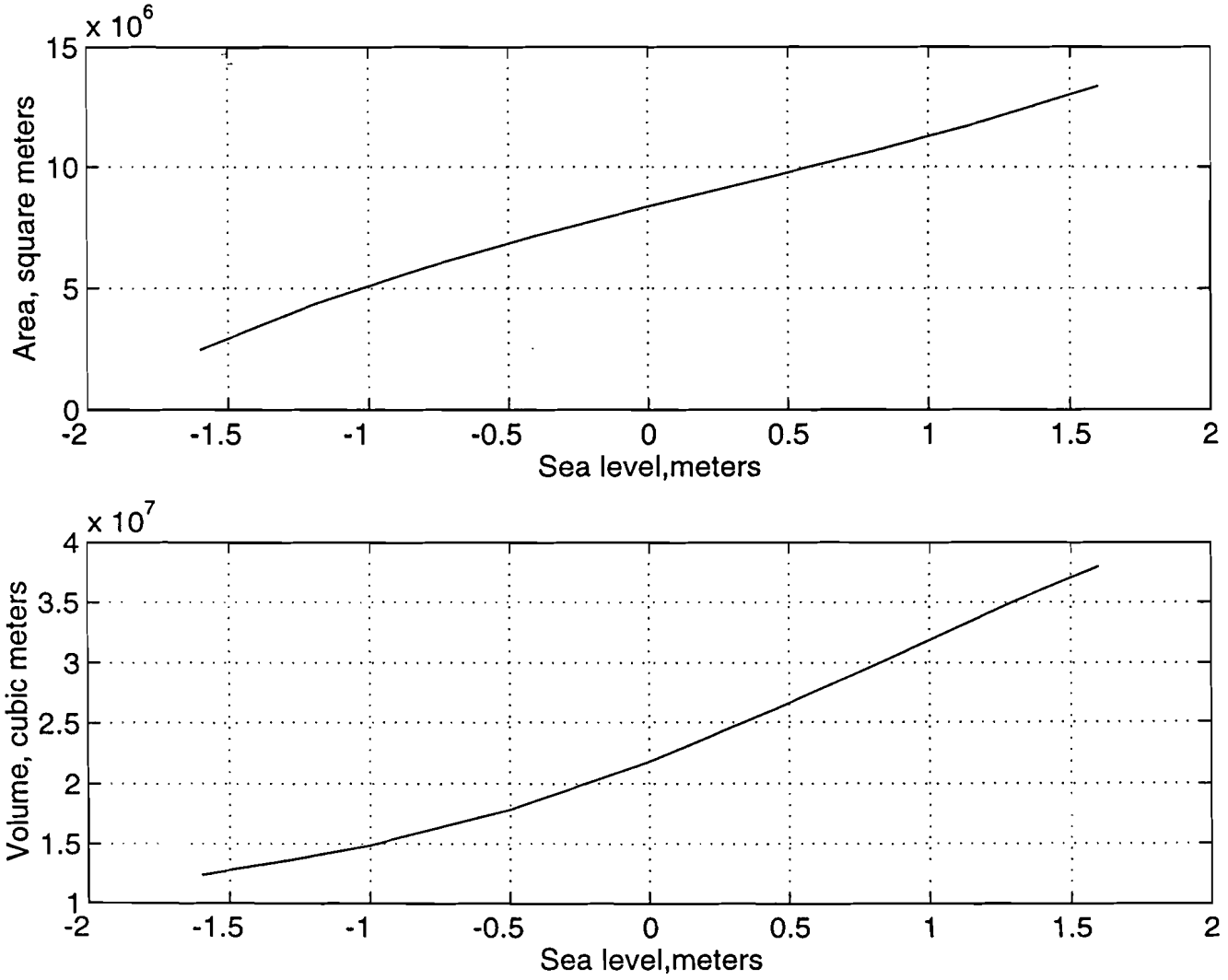

Fig 14. Hypsographic curve of Mtwapa creek showing: (a) Surface area as a function of sea level and (b) Volume of water contained within the creek as a function of sea level.

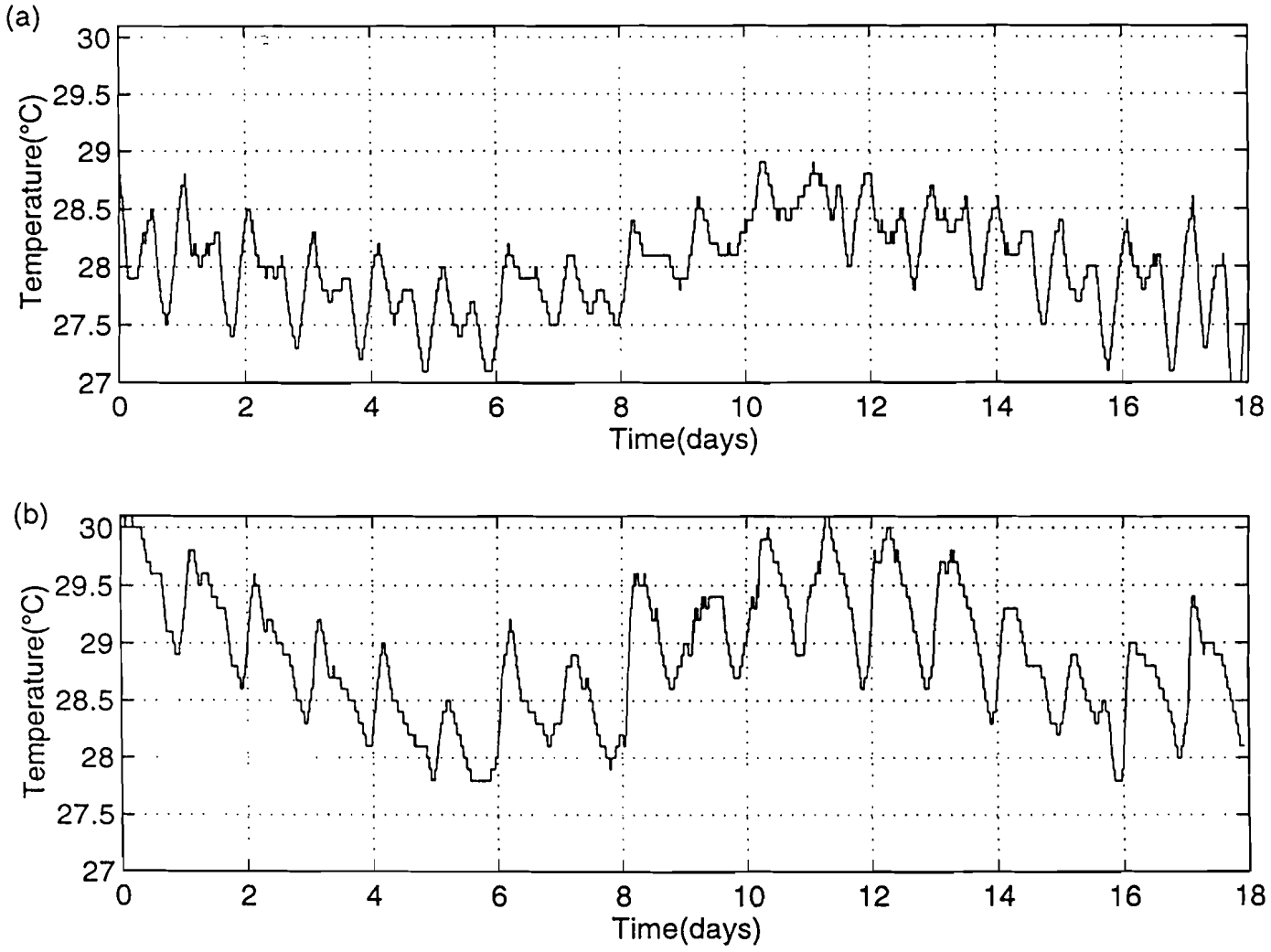

Fig 15. Time series of Temparature variations recorded at : (a) Claudio, January 1997 and (b) Creek, January 1997

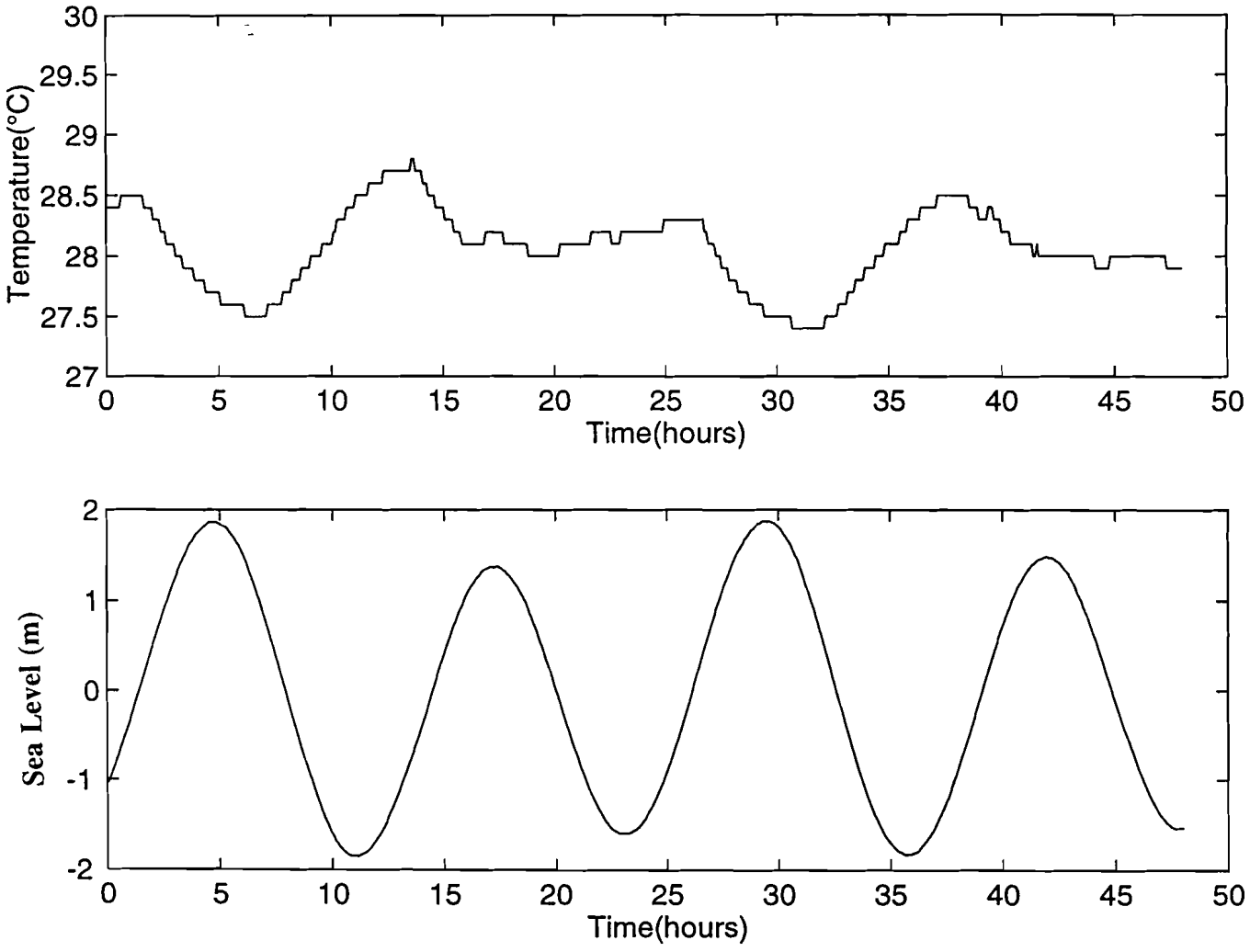

Fig 16a. Comparison of sea levels and water temperatures at Claudio station
Start time- 10 January 1997, 0000 hrs,.

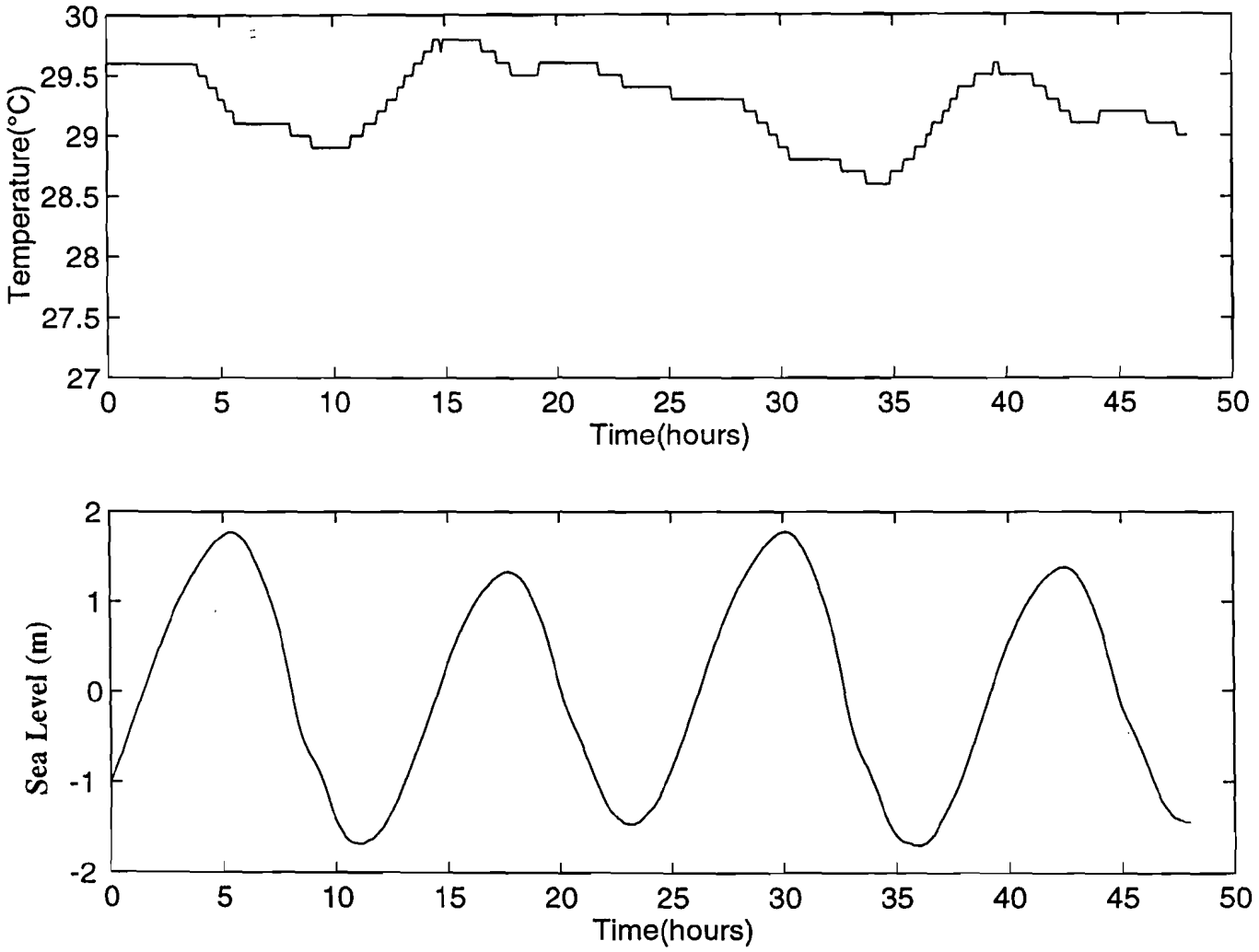

Fig 16b. Comparison of sea levels and water temperatures at Creek station
Start time-10 January 1997, 0000 hrs.

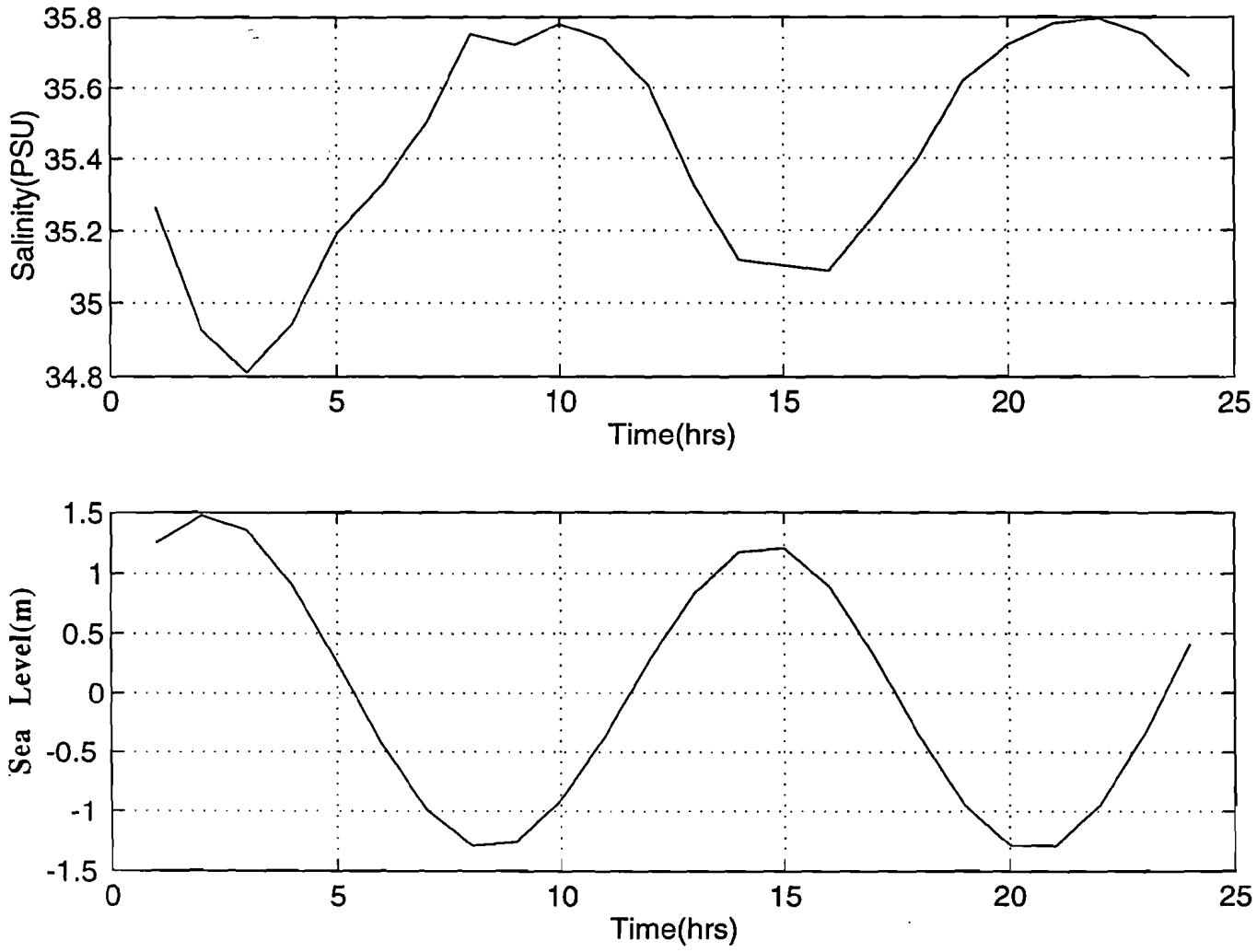

Fig 17. Hourly salinity variations at Claudio in comparison with Sea levels September, 1997

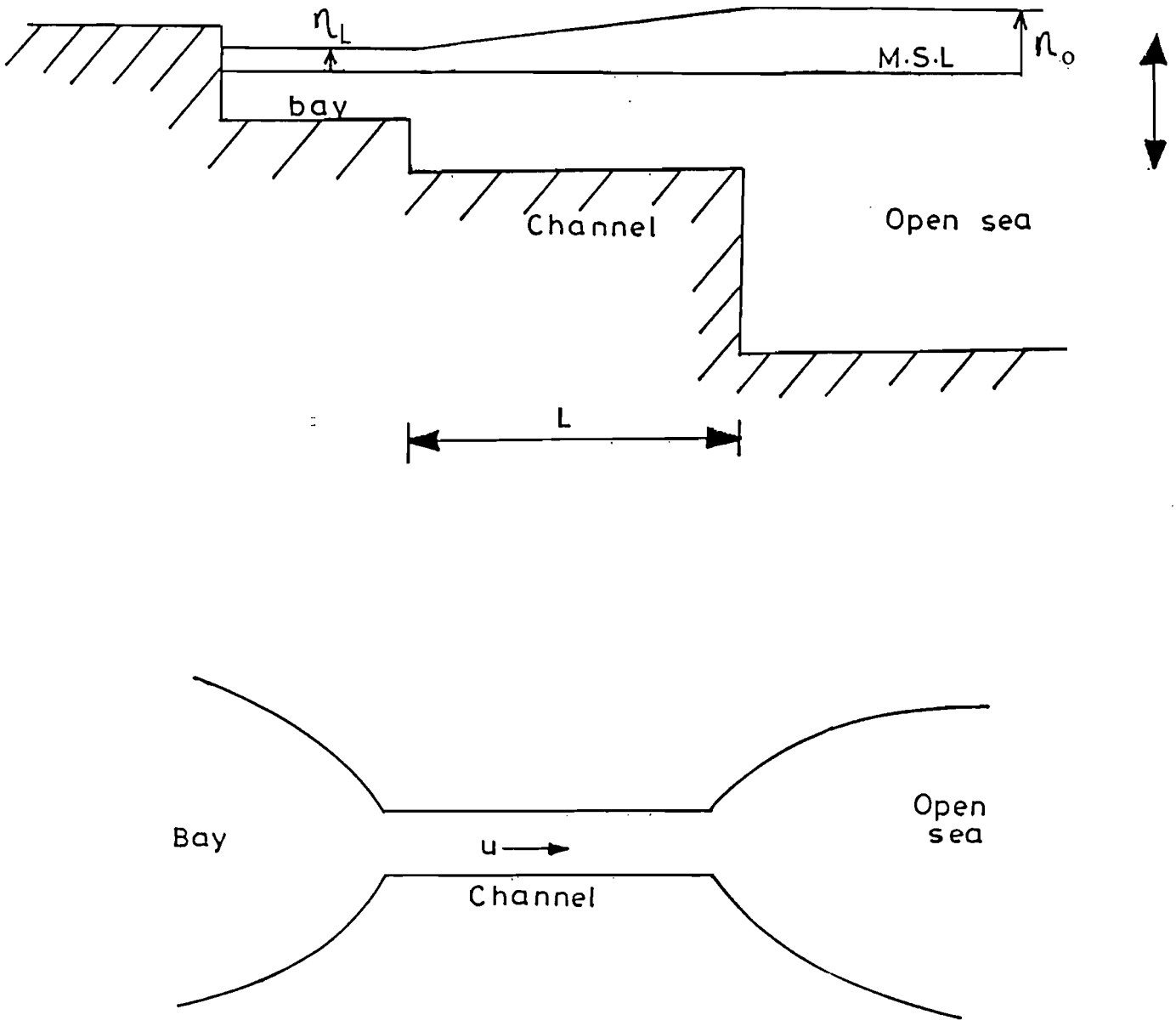

Fig 18. Assumed geometry of a lagoon connected to the ocean by a long narrow channel

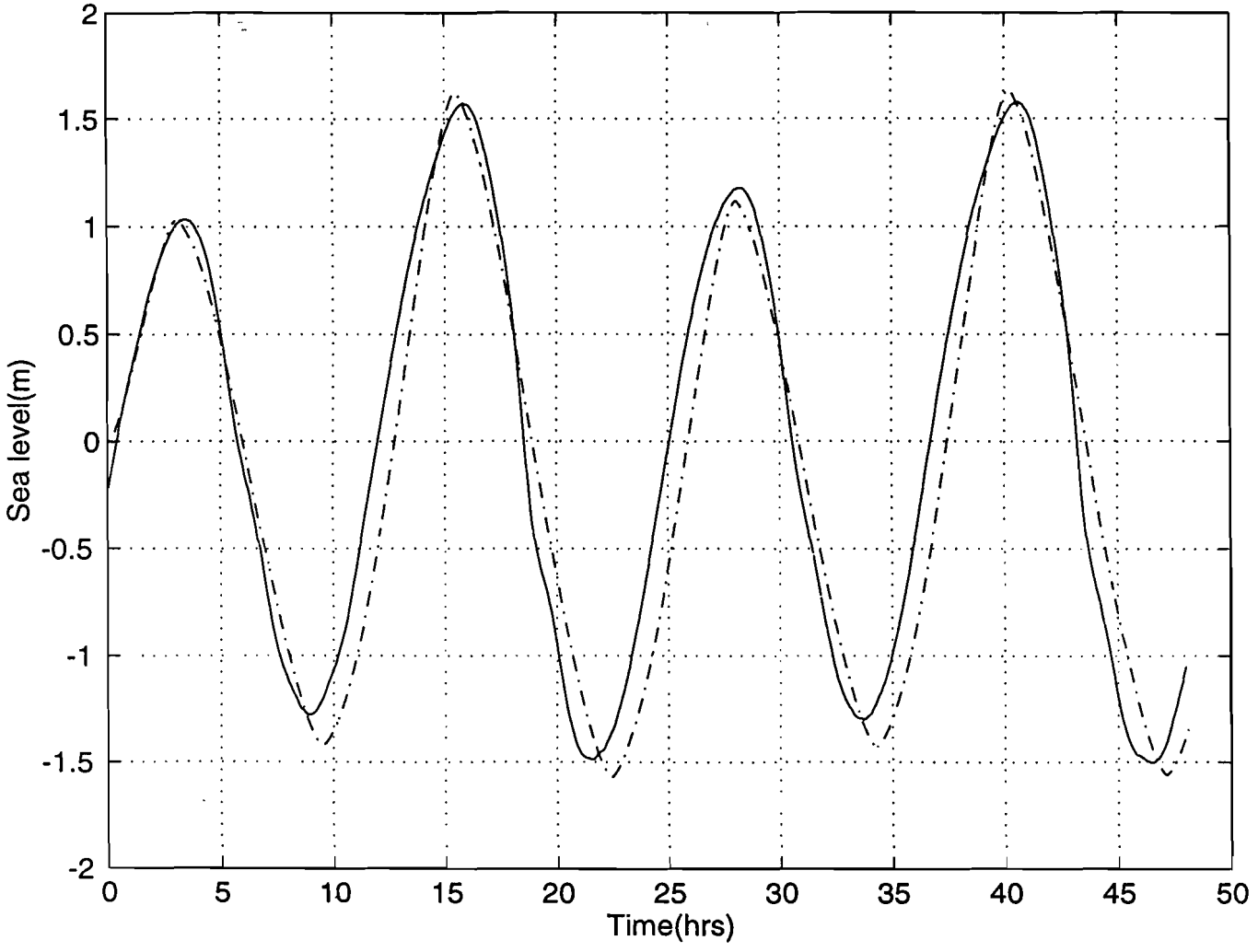

Fig 19. Comparison of observed (__) and predicted (-.-.) Sea levels at the Creek station.